

IBIA: Bayesian Inference via Incremental Build-Infer-Approximate operations on Clique Trees.

Shivani Bathla
Vinita Vasudevan

EE13S064@EE.IITM.AC.IN
VINITA@EE.IITM.AC.IN

Department of Electrical Engineering, IIT Madras, Chennai 600036

Abstract

Exact inference in Bayesian networks is intractable and has an exponential dependence on the size of the largest clique in the corresponding clique tree, necessitating approximations. Techniques for approximate inference typically use iterative BP in graphs with bounded cluster sizes. We propose an alternative approach for approximate inference based on an incremental build-infer-approximate (IBIA) paradigm. In the build stage of this approach, bounded-clique size partitions are obtained by building the clique tree (CT) incrementally. Nodes are added to the CT as long as the sizes are within a user-specified clique size constraint. Once the clique size constraint is reached, the infer and approximate part of the algorithm finds an approximate CT with lower clique sizes to which new nodes can be added. This step involves exact inference to calibrate the CT and a combination of exact and approximate marginalization for approximation. The approximate CT serves as a starting point for the construction of CT for the next partition. The algorithm returns a forest of calibrated clique trees corresponding to all partitions. We show that our algorithm for incremental construction of clique trees always generates a valid CT and our approximation technique automatically maintains consistency of within-clique beliefs. The queries of interest are prior and posterior singleton marginals and the partition function. More than 500 benchmarks were used to test the method and the results show a significant reduction in error when compared to other approximate methods, with competitive runtimes.

1. Introduction

Bayesian Network (BN) based algorithms have been used for probabilistic inference in a wide variety of applications. Methods for exact inference include variable elimination (Dechter, 1999), belief propagation (BP) on join trees (Lauritzen & Spiegelhalter, 1988; Shenoy & Shafer, 1986) and weighted model counting (Darwiche, 2001; Chavira, Darwiche, & Jaeger, 2006; Chavira & Darwiche, 2008; Sang, Beame, & Kautz, 2005; Dudek, Phan, & Vardi, 2020; Dilkas & Belle, 2021). Exact inference is known to be $\#P$ complete (Koller & Friedman, 2009), being time and space exponential in the treewidth of the graph. Even some relatively small BNs have a large treewidth, necessitating approximations. Although approximate inference with error bounds is also NP hard (Roth, 1996), many of the approximation techniques work well in practice.

A widely used method of approximation is the “loopy belief propagation” (LBP) algorithm, which is based on using Pearl’s message passing (MP) algorithm for trees iteratively on networks with cycles (Frey & MacKay, 1998; Murphy, Weiss, & Jordan, 1999). The converged solution of LBP was shown to be a fixed point of the Bethe free energy (Yedidia, Freeman, Weiss, et al., 2000; Heskes, 2003). Alternatives to the basic LBP include fractional BP (FBP) (Wiegerinck & Heskes, 2003), the tree-reweighted BP (TRWBP) (Wainwright,

Jaakkola, & Willsky, 2003), mean field (MF) (Winn, Bishop, & Jaakkola, 2005) and expectation propagation (EP) (Minka, 2001, 2004), all of which can also be viewed as minimization of a particular information divergence measure (Minka, 2005). Other variants include message-scheduling based on residuals (Elidan, McGraw, & Koller, 2006) and belief propagation neural network (BPNN) (Kuck et al., 2020), that contains an iterative layer that outputs messages of the BP algorithm and a Bethe free energy layer that performs regression on beliefs to obtain the partition function. The two issues in these methods are convergence and accuracy of the converged solution. The iterative message passing algorithm is not guaranteed to converge in general, but there are alternative methods of solution that guarantee convergence (Yuille & Rangarajan, 2002; Heskes, 2006). LBP and its variants have been empirically found to give good solutions in many cases, especially if the influence of the loops is not very large. The accuracy can be improved by performing iterative belief propagation between clusters of nodes or regions (Yedidia et al., 2000; Dechter, Kask, & Mateescu, 2002; Yedidia, Freeman, & Weiss, 2005; Mooij & Kappen, 2007). These algorithms are known as the generalized belief propagation (GBP)/cluster variation(CVM)/region graph based methods. The converged solutions of GBP are shown to be the fixed points of the Kikuchi free energy (Kikuchi, 1951). The size of the clusters or regions can be used to trade-off accuracy for computational efficiency and the converged solution depends on the choice of regions. There are several approaches to identification of regions. Methods proposed in Gelfand and Welling (2012), Welling, Minka, and Teh (2005), Mateescu et al. (2010) use structural information of the graph to bound the size of the clusters. Methods like region pursuit (Welling, 2004; Hazan, Peng, & Shashua, 2012), cluster pursuit (Sontag et al., 2008) and triplet region construction (TRC) (Lin, Neil, & Fenton, 2020) use factor based information. Although factor-based partitioning is preferable, it involves multiple rounds of region reconstruction/addition and belief propagation, which can become expensive (Welling, 2004). To reduce this computational cost, localized computations are used to add clusters to the outer region (Sontag et al., 2008; Lin et al., 2020). In Sontag et al. (2008), several potential clusters are scored based on potential improvement of a lower bound using pairwise and joint factors. A problem is huge number of candidate clusters. TRC uses differences in conditional entropy computed using pseudo-marginals to identify interaction triplets.

Another technique for approximate inference based on BP is the use of approximate factorized messages. Algorithms in this class include mini-bucket elimination (MBE) (Dechter & Rish, 1997, 2003) and weighted MBE (WMB) (Liu & Ihler, 2011; Forouzan & Ihler, 2015; Lee et al., 2020), mini-clustering (MC) (Mateescu et al., 2010) and iterative join graph propagation (IJGP) (Dechter et al., 2002; Mateescu et al., 2010). These algorithms trade off accuracy and complexity by limiting the scope of the factors in a mini-bucket or a mini-cluster to a preset bound (*ibound*). The key idea in these algorithms is the following - instead of using the sum/max operator after finding the product of the factors in a cluster, they migrate the sum/max operator to each mini-cluster to give an upper bound on the beliefs and the partition function. WMB uses weighted factors and the Holder inequality to get the approximate messages. MC uses mini-bucket heuristics to partition clusters in a join-tree into mini clusters. IJGP uses iterative belief propagation in a join graph (rather than tree) with mini-bucket heuristics to bound cluster sizes. Most of the algorithms use scope-based partitioning of buckets or clusters. As is the case with region selection, scope based partitioning can be carried out in many ways and each partition could result in a

different bound. Like the cluster and region pursuit methods to identify optimum regions, factor based information to find clusters has been explored in Rollon and Dechter (2010) and Forouzan and Ihler (2015). In Rollon and Dechter (2010), a greedy heuristic based on a local relative error is used find a partition that best approximates the bucket function. In Forouzan and Ihler (2015), after using WMB on a join graph to get initial beliefs, mini-buckets within a bucket are considered for merging based on a score that is computed using localized change in messages. When compared to the method in Sontag et al. (2008), the search for candidate region is more structured and well defined.

Another approach is to perform inference on progressively more complex networks in each iteration. In a series of papers, Choi and Darwiche (Choi, Chan, & Darwiche, 2005; Choi & Darwiche, 2006, 2007, 2008) propose the relax-compensate-recover scheme which starts with a simpler network obtained by deleting edges, duplicating nodes and adding auxiliary evidence nodes along with some consistency conditions. The belief propagation is done iteratively with some edges added in each new iteration, in the compensate and recover phase. More generally, the relax-recover-compensate method computes beliefs by relaxing equivalence constraints and recovers by adding some of the constraints (Choi & Darwiche, 2010).

All of these methods use some kind of partitioning to get bounded cluster sizes along with iterative BP for inference. The general method to improve accuracy is to use beliefs obtained from relaxed structures to get better partitions. This procedure is done iteratively, to identify better clusters. Our approach to partitioning with bounded clique sizes is different. It is based on incremental build-infer-approximate (IBIA) paradigm, that has the following steps.

- The BN has a natural topological ordering of nodes. We denote the nodes that have no parents as primary inputs (PI) to the network. Starting with the PIs, we propose a novel algorithm to construct the CT incrementally, adding as many nodes as possible until a preset bound (mcs_p) on the clique size is reached. All the nodes that have been added to the CT belong to a partition of the graph. We show that our algorithm produces a valid CT containing only maximal cliques and satisfying RIP.
- When the bound is reached, the CT is first calibrated using the standard join tree message passing algorithm (Koller & Friedman, 2009). The CT contains two sets of variables - variables that are parents to nodes that have not yet been added (we denote these nodes as *interface nodes*) and other variables (*non-interface nodes*). Using a mutual information based metric, non-interface variables that have the least correlation with the interface variables are identified. The variables are summed out using a combination of exact and approximate marginalization until the clique size is reduced to a lower value mcs_{im} , thus allowing for addition of new nodes. This approximate CT is used as the starting point for incremental construction of the CT for the next partition. The process is continued until all nodes in the BN are added. The algorithm returns an ordered set of partitions and a forest of CTs (CTFs) for each partition.
- We show that our approximation algorithm maintains consistency of within-clique beliefs.
- We show that an estimate of the partition function can be obtained using the normalization constant of cliques in the last partition.

- We show that the prior singleton marginals are consistent across partitions and can be obtained from any partition. The posterior singleton marginals are also consistent once all the evidence variables have been added to the CT. The posterior singleton marginals of the remaining variables are updated via a heuristic back-propagation algorithm.

Additionally,

- IBIA is non-iterative in the sense that it does not require BP to run until convergence or multiple rounds of BP on progressively “harder” structures.
- It partitions the network and return a forest of CTs, but the partitioning is not done a priori at the network level. It occurs naturally as a part of the algorithm and is based on factor information. Belief propagation (BP) is required before approximation, but it is run locally within a partition.
- The trade-off between accuracy and complexity can be achieved using two parameters, mcs_p and mcs_{im} . mcs_p controls the maximum clique size in a partition and hence the time and space complexity of inference within a partition. mcs_{im} controls the number of partitions. If mcs_{im} is smaller, a larger number of nets can be added in each partition, thus reducing the number of partitions. However, the approximation could be more aggressive, especially in networks with long cycles that span several topological levels.
- Since we build the clique tree incrementally, the proposed framework allows the flexibility of incorporating incremental addition/deletions to portions of the network.
- Exact inference is used in the CTs corresponding to various partitions. The approximation is due to the approximate starting CTs from which the CTs for a partition are built. Moreover, approximation is performed only when clique sizes cannot be reduced by exact marginalization alone. As a result, the prior beliefs in the first partition are always exact. If the evidence and query is in the first partition, it is also exact. Even with partitioning, error could be zero if a sufficient number of non-interface variables can be marginalized out exactly.

We have compared the results of our algorithm with other approximate inference methods like FBP, TRWBP, WMB and IJGP for 500+ benchmarks. The focus of this paper is “deterministic” approximate inference as opposed to sampling based techniques. However, we have compared our results with results obtained using Gibbs sampling implemented in libDAI (Mooij, 2010a) and wherever possible, with the results reported in Gogate and Dechter (2011).

Exact inference in partitioned networks has been explored in Xiang, Poole, and Beddoes (1993) and Xiang and Lesser (2003), but the partitioning is done at the network level making it difficult to ensure bounded clique sizes in each partition. Incremental methods for CT modification have been explored in some previous works (Draper, 1995; Darwiche, 1998; Flores, Gámez, & Olesen, 2002). In Draper (1995), incremental addition of links is performed by first forming a cluster graph using a set of rules and then converting the cluster graph into a junction tree. Although several heuristic-based graph transformations

are suggested, a difficulty is to choose a set of heuristics, so that clique size constraints are met. Also, there is no specific algorithm to construct the CT. A preferable method would be to make additions to an existing CT. Dynamic reconfiguration of CTs is explored (Darwiche, 1998), but it is specific to evidence and query based simplification. A more general method has been proposed in Flores et al. (2002). Here, the minimal section of the clique tree that needs modification is identified using the Maximal Prime Subgraph Decomposition (MPSD) (Olesen & Madsen, 2002) of the BN. Based on the moralized graph, the junction tree is converted into another graphical representation called the MPD join tree. We have a more detailed comparison with the partitioning and incremental compilation methods in section VII.

The rest of this paper is organized as follows. Section 2 provides background and notation. We describe the proposed overall algorithm in Section 3, the proposed incremental approach for building clique tree models in Section 4, the approximation technique in Section 5 and the inference of marginals and the partition function in Section 6. Section 7 contains a discussion of our algorithm and comparison with related work. Section 8 has the results. Finally, we present our conclusions in Section 9.

2. Background

This section has the notation and the definitions related to inference on Bayesian networks. Throughout the paper, we use the terms clique tree and join tree interchangeably. Also, as is common in the literature, we use term C_i as a label for the clique as well as to denote the set of variables in the clique.

Definition 1. Bayesian Network (BN): The Bayesian network is a directed acyclic graph (DAG), \mathcal{G} . Its nodes represent random variables $\mathcal{X} = \{X_1, X_2, \dots, X_n\}$ with associated domains $D = \{D_{X_1}, D_{X_2}, \dots, D_{X_n}\}$. It has directed edges from a subset of nodes $\text{Pa}_{X_i} = \{X_k, k \neq i\}$ to X_i , representing a conditional probability distribution (CPD) $P_i = P\{X_i | \text{Pa}_{X_i}\}$. The BN represents the joint probability distribution (JPD) of \mathcal{X} , given by $P(\mathcal{X}) = \prod_{i=1}^n P_i$.

Definition 2. Moralized graph ($\mathcal{M}(\mathcal{G})$): It is an undirected graph over \mathcal{X} that contains an edge between two nodes X_i and X_j if (a) there is a directed edge in either direction between X_i and X_j in \mathcal{G} or (b) X_i and X_j are parents of a node in \mathcal{G} .

Definition 3. Chordal graph (\mathcal{H}): It is an undirected graph that contains no cycle of length greater than three.

It is obtained from $\mathcal{M}(\mathcal{G})$ by triangulating all cycles of length greater than three.

Definition 4. Join tree or Clique tree (CT) (Koller & Friedman, 2009): The CT is a hypertree with nodes $\{C_1, C_2, \dots, C_n\}$ that are the set of cliques in \mathcal{H} . An edge between C_i and C_j is associated with a sepset $S_{i,j} = C_i \cap C_j$. The CT satisfies the following

- (a) All cliques are maximal cliques i.e., there is no C_j such that $C_j \subset C_i$.
- (b) Each factor P_i is associated with a single node C_i such that $\text{Scope}(P_i) \in C_i$.
- (c) It satisfies the *running intersection property* (RIP), which states that for all variables X , if $X \in C_i$ and $X \in C_j$, then X is present in every node in the unique path between C_i and C_j .

Exact inference in a CT is done using the belief propagation (BP) algorithm (Chapter 10 of Koller & Friedman, 2009) that is equivalent to two rounds of message passing along the edges of the CT, an upward pass (from the leaf nodes to the root node) and a downward pass (from the root node to the leaves). Following this each node has an associated belief $\beta(C_i) = P(C_i) = \sum_{\mathcal{X} \setminus C_i} P(\mathcal{X})$.

A calibrated CT is defined as follows.

Definition 5. Calibrated CT (Koller & Friedman, 2009): Let $\beta(C_i)$ and $\beta(C_j)$ denote the beliefs associated with adjacent cliques C_i and C_j . The cliques are said to be calibrated if

$$\sum_{C_i \setminus S_{i,j}} \beta(C_i) = \sum_{C_j \setminus S_{i,j}} \beta(C_j) = \mu(S_{i,j})$$

Here $S_{i,j}$ is the sepset corresponding to C_i and C_j and $\mu_{i,j}$ is the associated belief. The CT is said to be calibrated if all pairs of adjacent cliques are calibrated.

In a calibrated CT, adjacent cliques agree on the marginals. Hence, the marginal of a variable or a set of variables can be computed from any clique containing the variables. $P(\mathcal{X})$ can be written in terms of the sepset and clique beliefs as follows:

$$P(\mathcal{X}) = \frac{\prod_{i \in \mathcal{V}_T} \beta(C_i)}{\prod_{(i,j) \in \mathcal{E}_T} \mu(S_{i,j})}$$

where \mathcal{V}_T and \mathcal{E}_T are the set of nodes and edges in the CT.

The complexity of exact inference is space and time exponential in the treewidth, defined as follows.

Definition 6. Treewidth: The treewidth is one less than the minimum possible value of the maximum clique size, over all possible triangulations of the moralized graph.

The queries we are interested in are the prior and posterior marginals (MAR_p , MAR_e) and the partition function (PR). Definitions related to these are the following.

Definition 7. Primary inputs (PI): The BN allows for a natural topological ordering of nodes. We use PI to denote the set of nodes that do not have any parents.

Definition 8. Evidence Variables (E): Evidence variables are set of instantiated variables.

Definition 9. Partition function (PR): It is defined as the probability of evidence $P(E)$.

Figure 1 illustrates the steps involved in converting a BN into a CT model that can be used for inference. The BN is first converted to a moralized graph by removing edge orientations and adding pairwise edges between parents of each node, marked in the figure using dashed red lines. Next, the *chordal* completion of the moralized graph is obtained by adding edges to break all loops of size greater than three. In the figure, loop $d - b - e - f$ is broken by adding a chord between nodes d and e . Finally, the CT is formed with the maximal cliques of the chordal graph as nodes. Each factor P_i is assigned to a clique containing its scope, after which two rounds of message passing is performed to get the calibrated clique and sepset beliefs. Since finding a triangulation in which the size of the largest clique is equal to the treewidth is NP-hard, several heuristics have been proposed. In this paper, we have used variable elimination along with the min-fill heuristic (Koller & Friedman, 2009).

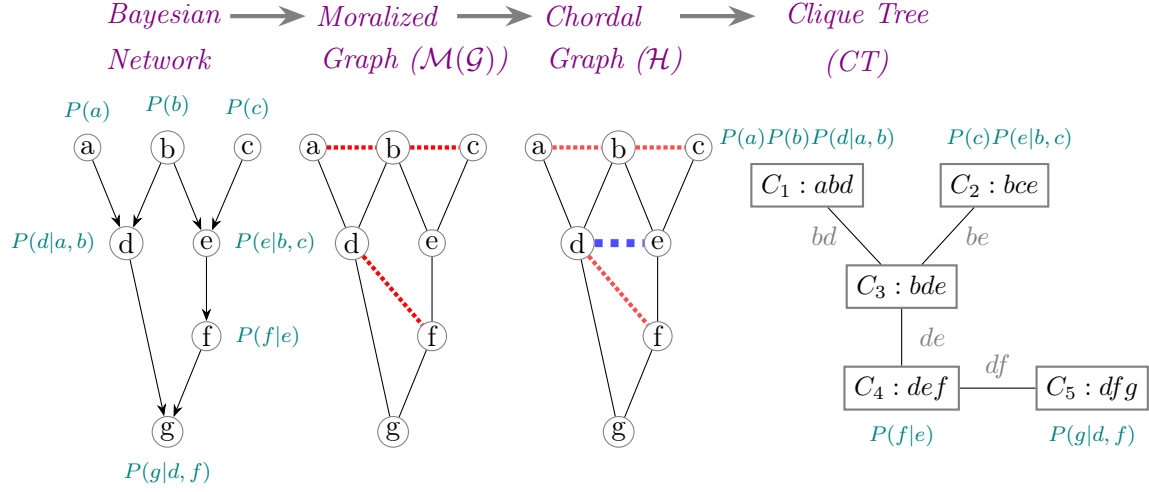


Figure 1: Compilation of a BN into a Clique Tree. The dotted red lines are the moralizing edges between parents, and the dashed blue lines are the fill-in edges introduced during triangulation. The sepset variables corresponding to each edge in the clique tree are marked in gray and the factors for each clique are shown in teal color.

3. Main Algorithm

The input BN could have disjoint DAGs. Hence, we use the term *Clique Tree Forest* (CTF) to denote the collection of corresponding CTs. Each connected DAG $\mathcal{G} \in \text{BN}$ is built, inferred and approximated separately. Our aim is to partition each DAG so that the maximum size of the cliques in the CTs corresponding to each partition is bounded. We define the clique size cs as follows

Definition 10. Clique size (cs): The size of the clique C_i (cs_i) is defined as

$$cs_i = \log_2 \left(\prod_{\forall v \in C_i} |D_v| \right)$$

where $|D_v|$ is the cardinality or the number of states in the domain of the variable v .

Based on this, we define a parameter mcs_p to denote the maximum permissible clique size in any partition. The CTF for each DAG is constructed incrementally and when the maximum clique size reaches mcs_p , the CTF is approximated until the maximum clique size is $mcs_{im} < mcs_p$. This is the starting point for the next partition. The process is continued until all nodes in the BN are added to the CTFs.

Algorithm 1 gives the main steps in our inference algorithm. The inputs to the algorithm are the BN, mcs_p , mcs_{im} and the map between evidence variables and their corresponding states. It returns the posterior singleton marginals MAR_e and the partition function (PR) if evidence variables are present and the prior singleton marginals MAR_p if there are no evidence variables.

Algorithm 1 InferenceEngine ($G, mcs_p, mcs_{im}, E, evidMap$)

Input: BN : Bayesian Network
 mcs_p : Maximum clique size limit for the partition CTF
 mcs_{im} : Maximum clique size limit for the approximated CTF
 E : Boolean variable indicating presence of evidence
 $evidMap$: Map of evidence variables and corresponding states $\langle ev : ev_{state} \rangle$

Output: MAR : Map of marginal probabilities of nets in BN
 PR : Probability of evidence

```

1: Initialize:
    $MAR = \langle \rangle$                                 ▷ Map  $\langle net : margProb \rangle$ 
    $PR = 1.0$                                     ▷ Probability of evidence
    $S_{eg} = \{ev \mid ev \in evidMap\}$            ▷ Set of all evidence variables
    $L_{CTF} = []$                                    ▷ List of  $CTF$  for each DAG
    $L_{IL} = [\langle \rangle]$                                 ▷ List of interface links for each DAG
    $LQ_e = []$                                     ▷ List containing last partition in which new evidence variables are added for each DAG

2: Simplify BN using steps discussed in Sec. 8.2.4
3:  $L_G \leftarrow$  List of connected DAGs in simplified BN
4: for  $G \in L_G$  do
5:   Initialize:  $CTF_G = []$ 
      $PI = \{\text{Nets in } G \text{ with zero in-degree}\}$ 
      $S_e = S_{eg}.\text{pop evidence variables in } G$            ▷ Set of evidence variables in  $G$ 
      $CTF = \{\text{Disjoint Cliques over } PI\}$              ▷ Clique Tree Forest
      $G.\text{remove}(PI)$                                      ▷ Remove  $PI$  and its outgoing edges from  $G$ 
      $S_e.\text{remove}(PI \cap S_e)$                          ▷ Remove evidence variables added to the  $CTF$ 
      $PartN = 1$                                          ▷ Partition Index
      $Q_e = 0$                                            ▷ Last partition containing evidence variables
      $LT = []$                                            ▷ List of links between input and approximate cliques
      $N_{act} \leftarrow$  Nets in  $G$  with zero in-degree     ▷ Active nets
6:   while  $G.\text{size} \neq 0$  do
7:     ▷ Add nets and update  $CTF$ 
8:      $N_a \leftarrow \emptyset$                                ▷ Set of nets added to  $CTF$ 
9:      $IV \leftarrow \emptyset$                                ▷ Interface nets
10:    while  $N_{act} \neq \emptyset$  do
11:       $N_i \leftarrow N_{act}.\text{pop nets with min. topological level}$ 
12:       $CTF, N_a \leftarrow \text{BuildCTF}(CTF, N_i, mcs_p, S_e)$ 
13:       $G.\text{remove}(N_a)$                                      ▷ Delete  $N_a$  and outgoing edges in  $G$ 
14:       $S_e.\text{remove}(N_a \cap S_e)$                          ▷ Remove evidence variables that are added to the  $CTF$ 
15:       $IV.\text{add parents of nets in } N_i \setminus N_a$        ▷ Interface variables
16:       $N_f \leftarrow$  Direct successors of  $N_a$  with zero in-degree in  $G$ 
17:       $N_{act}.\text{push}(N_f)$                                  ▷ Update the list  $N_{act}$ 
18:    end while
19:     $\beta, \mu \leftarrow$  Calibrate  $CTF$  using Belief Propagation
20:     $CTF_G.\text{append}(CTF)$ 
21:     $CTF, IM \leftarrow \text{ApproximateCTF}(CTF, IV, mcs_{im})$ 
22:    if  $E$  then
23:       $LT.\text{add}(IM)$ 
24:      if  $S_e == \emptyset \&\& Q_e == 0$  then  $LQ_e.\text{append}(PartN)$    ▷ All evidence variables have been added
25:    end if
26:     $PartN = PartN + 1$ 
27:  end while
28:   $L_{CTF}.\text{append}(CTF_G)$ 
29:   $L_{IL}.\text{append}(LT)$ 
30: end for
31: ▷ Use calibrated  $CTFs$  of the entire BN for queries
32: if  $\neg E$  then
33:    $MAR \leftarrow$  Compute prior marginals from calibrated  $CTFs$  in  $L_{CTF}$ 
34: else
35:    $PR = \text{ComputePF}(L_{CTF})$ 
36:    $MAR \leftarrow \text{GetPosteriorMAR}(LQ_e, L_{CTF}, L_{IL})$ 
37: end if
38: return  $MAR, PR$ 

```

The main steps in the Algorithm 1 are as follows. The line numbers in the following description refer to this algorithm. The BN and CPDs are first simplified based on evidence and other fixed states (line 2). The CTF for a DAG $G \in BN$ is built incrementally, starting with PIs in disjoint cliques (line 5). Each time a node is added to CTF, the node along with its outgoing edges is removed from the corresponding DAG, G . Therefore, if a node has zero in-degree in G , it means that all its parents have been added to the CTF. These nodes, termed *active nodes* (stored in N_{act}), are now ready for addition to the CTF (line 6). The iteration to build a CTF for a partition starts with the set of active nodes that have the lowest topological level (N_i). Evidence variables are prioritized for addition to the CTF. The set S_e tracks the set of evidence variables that are yet to be added. Nodes that are successfully added (N_a) to the CTF are removed from G and S_e , following which N_{act} is updated. Parents of nodes that could not be added ($N_i \setminus N_a$) are added to the set of interface nodes (IV). The iteration continues until N_{act} is empty (lines 7-19).

Algorithm 1 uses the following main functions.

- *BuildCTF* (described in Algorithm 3): This function is used to incrementally add nodes to the CTF under a given maximum clique size constraint mcs_p (line 13).
- *BeliefPropagation*: It is a standard exact inference method based on two-pass message passing algorithm (Chapter 10 of Koller & Friedman, 2009) that returns a calibrated clique and sepset beliefs (β, μ) (line 20).
- *ApproximateCTF* (described in Algorithm 4): This function approximates the calibrated CTF until the clique sizes reduce to a given threshold mcs_{im} . It also returns a table (IM) containing links between cliques in the approximate and input CTF (line 22). This table is used for belief update to get posterior marginals.

For each DAG $G \in BN$, the above functions are called iteratively until G is empty. If G is the i^{th} DAG in the BN , at the end of the iteration, we get an ordered set of partitions $\{Q_{i1}, Q_{i2}, \dots, Q_{in_i}\}$ along with their calibrated CTFs $\{CTF_{i1}, CTF_{i2}, \dots, CTF_{in_i}\}$ and links between CTFs of adjacent partitions $\{IM_{i1}, IM_{i2}, \dots, IM_{in_i}\}$ for G . The set of calibrated CTFs are added to the list L_{CTF} and the set of links are added to the list LT . This process is continued until a CTF is built for all DAGs in the BN .

We now have the calibrated CTFs for all the DAGs, which can be used for inference (lines 33-38). If there is no evidence, clique beliefs of the calibrated CTFs directly give the prior marginals. Otherwise, Algorithm 1 invokes the following functions.

- *ComputePF* (described in Algorithm 5): It computes the partition function.
- *GetPosteriorMAR* (described in Algorithm 7): Computes posterior marginals for all variables.

Each of these algorithms are described in detail in the following sections.

4. BuildCTF: Algorithm for incremental construction of CTF

In this section, we describe the methods used to incrementally construct clique trees. We first describe the algorithm and then show that the algorithm will always result in a valid CTF.

4.1 Modifying existing CTF to add a single net

Let us first consider the addition of a single net n with parent nodes p_1, \dots, p_m to an existing CTF. This will introduce moralizing edges between all pairs of parent variables, resulting in an additional clique C_n with scope equal to $[p_1, \dots, p_m, n]$ and an associated factor $P(n|p_1, \dots, p_m)$. The existing CTF now needs to be modified so that this clique can be added while ensuring that the CTF remains valid. The modifications required depend on the location of the parent nets (p_1, \dots, p_m) in the existing CTF. We first identify a minimal sub-graph of the CTF (SG_{min}) containing all the parent nodes. This is done by first identifying a subgraph containing the parents. Then, starting from the leaf nodes of the subgraph, cliques that contain the same set (or subset) of parents as their neighbors are removed recursively. Cliques in SG_{min} are impacted by the addition of the new net.

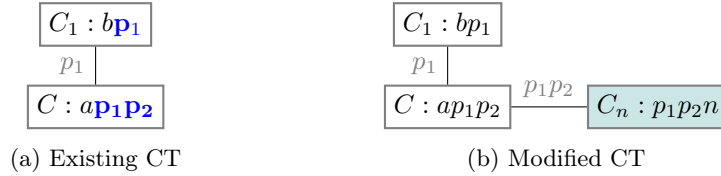


Figure 2: Case 1: Addition of a new net n with both parents in the same clique in the existing CT.

Based on the structure of SG_{min} , we identify three possible cases.

Case 1: SG_{min} has a single node. This will happen if all parents are contained in the same clique C . In this case, we connect C_n to C as shown in Figure 2. In case C is contained in C_n , C is replaced by C_n .

Case 2: SG_{min} is a set of disconnected cliques. If the parents belong to disconnected cliques C_1, \dots, C_j in CTF, C_n gets connected to C_1, \dots, C_j . An example is shown in Figure 3. Here SG_{min} has two disconnected cliques C_1 and C_2 and the addition of C_n connects them. Any non-maximal clique $\in \{C_1, \dots, C_j\}$ is replaced by C_n .

Case 3: SG_{min} is fully or partially connected. An example is shown in Figure 4a, where the cliques shaded in red form SG_{min} . If one or more subsets of parent variables belong to different cliques in the same CT, the addition of the new clique introduces moralizing edges between parents resulting in chordless loops in existing the chordal graph of the CT. These chordless loops need to be retriangulated. Figure 4a shows an example of such a case. In the example, chordless loops p_1abcp_2 and p_1dbcp_2 that are introduced need retriangulation, as shown in Figure 4b. The following steps are used to modify the CTF in this case.

Step 1: Construct a set S containing parent nodes and all nodes in the sepsets in SG_{min} . For the example, $S = \{p_1, p_2, a, d, b, c\}$.

Step 2: Find cliques $\in SG_{min}$ that contain nodes $\notin S$. These cliques are called *retained cliques*. In the example, C_3 is a retained clique.

Step 3: Find the modified clique tree ST' using the following steps.

Step 3.1: Construct a graph G_E as follows. The nodes of the graph are the nodes contained in the set S . The edges are obtained as follows. Corresponding to each clique C in

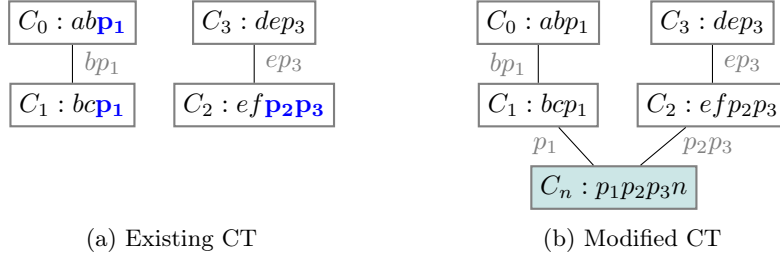


Figure 3: *Case 2*: Addition of a new net n , with parents in disconnected cliques.

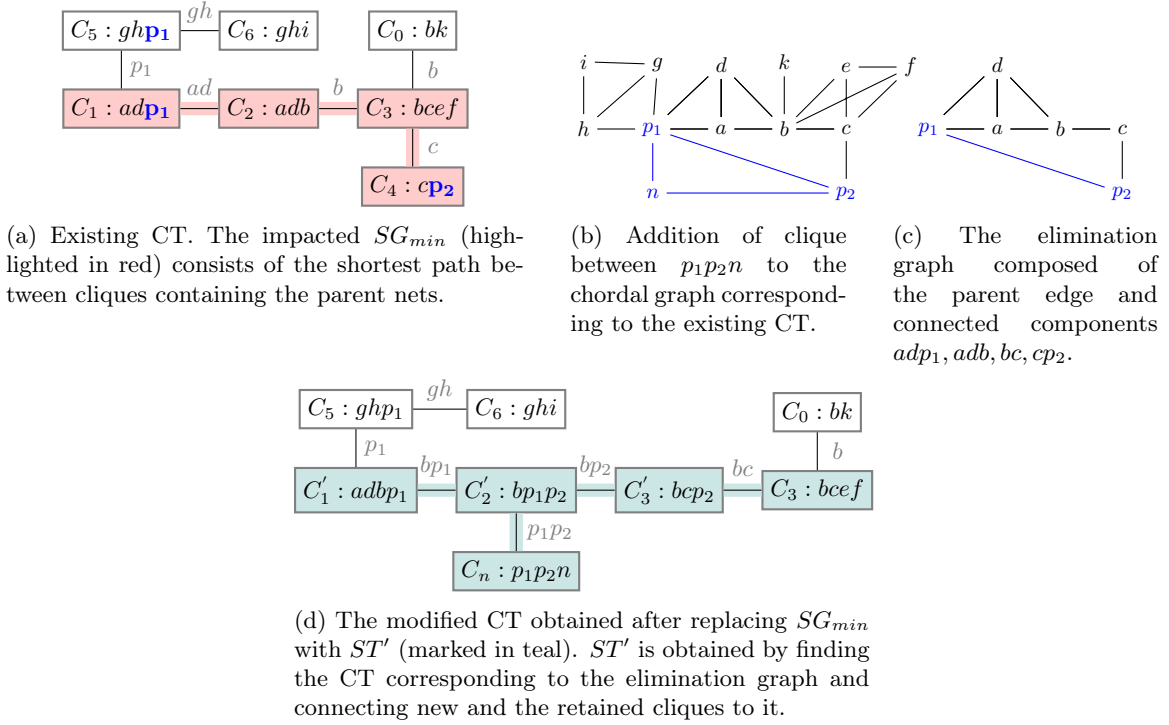


Figure 4: *Case 3*: Addition of a new net n , with parents in connected cliques.

SG_{min} , a clique $C_v = C \cap S$ is added to G_E . Finally, a moralizing edge is introduced between the parents. We call this graph the *elimination graph*. Figure 4c shows the elimination graph for the example. This is the graph that needs to be retriangulated.

- Step 3.2: Triangulate G_E and obtain the modified clique tree ST' .
- Step 3.3: Connect the new clique C_n to the clique C' in ST' that contains all parents. If $C' \subset C_n$, replace C' with C_n .
- Step 3.4: For each retained clique C , identify clique C' in ST' that contains $C \cap S$. Connect C to C' . If $C' \subset C$, replace C' with C . In the example, clique C_3 is connected to C'_3 .
- Step 3.5: The factors associated with cliques that are not retained are reassigned to cliques in ST' containing the entire scope of factors.

Step 4: Remove the impacted subgraph SG_{min} from CTF.

Step 5: Connect ST' to CTF via the set of cliques adjacent to SG_{min} in the existing CTF. Cliques in this adjacency set are reconnected to cliques in ST' that contain the corresponding sepset in the input CTF. For the example, the modified CT is shown in Figure 4d.

Algorithm 2 shows the steps for addition of a single node.

Algorithm 2 AddNode(n, C_n, SG_{min}, CTF)

Input: n : New net to be added
 C_n : New clique containing the node n and parent nodes
 SG_{min} : Minimal subgraph containing the parent nodes
 CTF : Existing CTF

Output: CTF : Modified CTF

```

1: if Case 1 or Case 2 then
2:   Connect  $C_n$  to parent cliques; Check Maximality
3: else
4:   Construct set  $S = \{\text{sepsets}(SG_{min}), p_1, \dots, p_m\}$ 
5:    $RC$ : List of retained cliques.
6:   ▷ Build Elimination Graph - Step 3.1, Case 3
7:    $G_E = \text{Graph}()$ 
8:    $G_E.\text{add\_clique}\{C \cap S\} \quad \forall C \in SG_{min}$ 
9:    $G_E.\text{add\_clique}\{p_1, \dots, p_m\}$ 
10:  ▷ Find  $ST'$  - Steps 3.2-3.5, Case 3
11:   $ST' \leftarrow$  Triangulate  $G_E$  and construct clique tree
12:  Connect cliques in  $RC$  to  $ST'$ ; check maximality; Reassign factors;
13:  Connect  $C_n$  to  $ST'$ ; check maximality
14:  ▷ Replace  $SG_{min}$  by  $ST'$ 
15:   $\text{Adj}(SG_{min}) \leftarrow$  Set of cliques adjacent to  $SG_{min}$  in  $CTF$ 
16:   $CTF.\text{remove}(SG_{min})$ 
17:  Connect  $ST'$  to  $\text{Adj}(SG_{min})$ 
18: end if
19: return  $CTF$ 

```

4.2 Modifying existing CTF to add multiple nodes with clique size constraints

As seen from lines 12-13 in Algorithm 1, in every iteration, we attempt to add a set of nodes to the CTF. Although these nodes can be added sequentially, it is more efficient to add nodes that have overlapping minimal subgraphs together, especially when SG_{min} is a connected graph. Algorithm 3 shows the main steps involved in modifying the CTF to add a set of nodes under a given maximum clique size constraint.

The line numbers in the following description refer to Algorithm 3. The addition of nodes belonging to the first two cases does not change the size of the existing cliques. We sequentially add as many of these nodes as possible to the CTF (lines 3-5). For nodes that fall under Case 3, we divide it into two sets depending on whether SG_{min} is connected or not. Nodes for which SG_{min} is partially connected are first added sequentially (line 6). For the remaining nodes, we use the following procedure to make sure that nodes which have overlapping SG_{min} are added together. This is more efficient since it avoids repeated formation and retriangulation of the same subgraph. We first find all cliques containing parents of these nodes, using which we find connected components of the clique tree. All nodes corresponding to a connected sub-tree are added together (lines 10-23). The procedure is similar to addition of a single node described in Algorithm 2, but now the elimination set

S will contain parents of all nodes in the subset as well as all the sepsets in the impacted subtree. If the maximum clique size in ST' is less than mcs_p , SG_{min} is replaced by ST' (lines 16-18). Otherwise, we choose a smaller subset N_s for addition and defer the remaining nodes to the next partition. We prioritize evidence variables while choosing the subset for addition (line 20). The reason for this is discussed in more detail in Section 6.2.1. Nodes in N_s are re-grouped based on overlapping paths, and the new groups are added to the list of subsets (lines 20-21). The iteration ends when the list becomes empty. Once the CTF is modified, we remove the evidence variables from the scope of cliques in CTF (line 24).

Algorithm 3 BuildCTF (CTF , N_i , mcs_p , S_e)

Input: CTF : Existing CTF
 N_i : Set of active nets to be added
 mcs_p : Maximum clique size limit for CTF
 S_e : Set of evidence variables

Output: CTF : Modified CTF
 N_a : Subset of N_i added to CTF

- 1: **Initialize:** $N_a = []$
- 2: \triangleright First add nodes whose parents belong to disconnected subgraphs. These are Case 1, Case 2 and some Case 3 nodes.
- 3: **for** $n \in N_i$ **do** $SG_{min} \leftarrow$ minimal subgraph containing parents of n
- 4: **if** $SG_{min}.is_connected$ **then** continue
- 5: $CTF' = \text{AddNode}(n, C_n, SG_{min}, CTF)$ \triangleright Use Algorithm 2 to add these nodes.
- 6: **if** $\max_clique_size(CTF') \leq mcs_p$ **then** $CTF = CTF'$; $N_a.add(n)$
- 7: $N_i.remove(n)$
- 8: **end for**
- 9: \triangleright Add remaining Case 3 nodes with connected overlapping subgraphs
- 10: $L_g \leftarrow$ Group nodes in N_i with overlapping SG_{min}
- 11: **while** $L_g \neq \emptyset$ **do**
- 12: $N_g = L_g.pop()$
- 13: $SG_{min} \leftarrow CTF.subgraph(\cup_{n \in N_g} SG_{min}[n])$ $\triangleright SG_{min}[n]$ is the minimal subgraph containing parents of n
- 14: $ST' \leftarrow$ Find modified subtree using lines 4-13 in Algorithm 2
- 15: \triangleright Add nodes if clique size constraints are met; else choose a subset
- 16: **if** $ST'.\max_clique_size \leq mcs_p$ **then**
- 17: Replace SG_{min} by ST' using lines 14-17 in Algorithm 2
- 18: $N_a.add(N_g)$
- 19: **else**
- 20: $N_s =$ Choose a subset of N_g for addition; Prioritize $N_g \cap S_e$ followed by nets with largest out-degree
- 21: Group nets in N_s with overlapping subgraphs and add to L_g
- 22: **end if**
- 23: **end while**
- 24: Remove evidence variables $N_a \cap S_e$ from CTF
- 25: **return** CTF, N_a

4.3 Data structures and Implementation

We use a hash table to perform these operations efficiently. As the CTF is constructed, we build a hash table that is indexed by the net and contains all the cliques in which the net is present. As a consequence, many of the steps involve a simple look-up and finding set intersections. These operations are fast as both nets and cliques are represented using integer identifiers.

We used the NetworkX library (Schult & Swart, 2008) to represent graphs. We use built-in library functions for finding connected components, subgraphs over a subset of nodes, and paths between nodes. We use our own implementations for operations like finding the maximal weight spanning tree and pre-order traversals.

4.4 Soundness of the algorithm

We now argue that if the input CTF is valid, incremental modification due to addition of a node or set of nodes using the algorithms described in sections 4.1 and 4.2 results in a valid CTF that satisfies the properties in Definition 4. The construction of the CTF starts with a set of disjoint nodes corresponding to the PIs, which is a valid CTF.

Proposition 1. *The modified CTF obtained using Algorithm 3 contains (possibly disjoint) trees i.e., no loops are introduced by the algorithm.*

Proof. As discussed in section 4.1, there are three cases. In all cases a new clique containing the node to be added and its parents is formed. In Case 1, it is connected to a single clique in the existing CTF. In Case 2, it connects disjoint trees. Therefore, in both cases, no loops are introduced and the resulting modified CTF consists of one or more disjoint trees.

In Case 3, a subset of new nodes that impact overlapping subgraphs are added together. The minimal subgraph SG_{min} containing all parents is removed from the CTF. For each new node, a new clique containing the node and its parents is formed. The presence of moralizing edges between parents of each node ensures that the elimination graph G_E is a connected graph. A clique tree ST' is obtained after triangulation of this graph. Each retained clique is re-connected to a single clique in ST' . Due to the moralizing edges, ST' also contains at least one clique containing all parents of a node, to which the new clique is connected. Hence, the resulting structure ST' continues to be a tree. ST' replaces SG_{min} and is connected to the CTF via the same set of cliques as SG_{min} . If SG_{min} is disconnected, replacement with ST' connects the corresponding clique trees via a single clique. Therefore, no loops are introduced and the modified CTF continues to have one or more disjoint trees. \square

Proposition 2. *After addition, the modified CTF contains only maximal cliques.*

Proof. In Cases 1,2, any clique $C \subset C_n$ is removed from the CTF. Similarly, in Case 3, the CTF obtained from the elimination graph, G_E , has only maximal cliques by construction. The final ST' is obtained after connecting retained and new cliques (lines 12-13, Algorithm 2), where there is an additional check for maximality. Cliques in CTF $\not\subset SG_{min}$ contain atleast one net that is not present in ST' , thus remain maximal. \square

Proposition 3. *Product of factors in the modified CTF gives the correct joint distribution.*

Proof. We start with a CTF consisting of PIs and corresponding factors, for which the joint distribution of nodes is correct. As new nodes are added, in all cases, we reassign the factors corresponding to cliques removed from the existing CTF to new cliques containing their scope. No change is made to factors assigned to the remaining cliques. The CPD of the new net n is assigned to C_n . Thus, the assignment remains valid after modification. \square

Proposition 4. *All CTs in modified CTF satisfy the running intersection property (RIP)*

Proof. Consider the chordal graph corresponding to the existing CTF. In Cases 1,2, this graph remains chordal after a clique is added between the new node and its parents. Thus, RIP is satisfied when C_n is connected to CTF with parents as sepsets.

For Case 3, let S_a denote the set of all variables in CTF, and S^c be the set $S_a \setminus S$. Recall that S is the set containing variables present in the elimination graph (line 4, Algorithm 2). The chordal graph corresponding to the existing CTF has a perfect elimination order such that no fill-in edges are introduced on elimination. Even after the addition of the moralizing edges between the parents (p_1, \dots, p_m) , variables in S^c can be eliminated in this order without adding any fill-in edges. Therefore, cliques containing these variables are retained as is in the final CTF. Elimination of variables in S could potentially introduce fill-in edges as they are a part of chordless loops introduced by the clique between the parents. The graph corresponding to the variables in S is precisely the elimination graph, which is re-triangulated (line 11, Algorithm 2). The corresponding clique tree is therefore valid by construction. The modified subtree ST' satisfies RIP because cliques are connected such that the sepsets contain all nets in the intersection with S (lines 12-13, Algorithm 2). The CTF obtained after replacing SG_{min} with ST' satisfies RIP because ST' is reconnected such that sepsets are preserved (lines 14-17, Algorithm 2). \square

Theorem 1. *The modified CTF obtained after addition of one or more nodes using Algorithms 2 and 3 is a valid CTF*

Proof. Based on Propositions 1 - 4, the modified CTF satisfies all the properties to ensure that it contains a set of valid CTs. \square

5. Infer and Approximate CTF

Algorithm 3 returns a CTF in which one or more cliques have the maximum allowed size mcs_p . To allow for the addition of new nodes, this CTF is approximated so that the maximum size of the cliques is a lower value mcs_{im} . Since this approximation is made based on the factors (and not based on the structure of the BN), the CTF is first calibrated using the standard belief propagation algorithm (Chapter 10 of Koller & Friedman, 2009) for exact inference and the clique and sepset beliefs (β, μ) are inferred. In the presence of evidence, un-normalized clique beliefs are used. After calibration, all cliques in a CT will have the same normalization constant, which is equal to the probability of evidence states added to the CT. If no evidence variables are present, the normalization constant is one and the cliques beliefs represent the joint probability distribution of the variables in the clique.

Let CTF_{in} denote the calibrated CTF that needs to be approximated. We classify the variables in CTF_{in} into *interface* and *non-interface* variables as follows:

Definition 11. Interface variables: Nodes in CTF_{in} with successors that have not been added to CTF_{in} .

Definition 12. Non-interface variables: Nodes in CTF_{in} that are not interface variables.

Algorithm 4 contains the algorithm used for the approximation. CTF_{in} and the list of interface variables (IV) serve as the input to the approximation algorithm. Non-interface variables are stored in the list NIV . Our approximation strategy is to reduce the size of the cliques by summing out some of the non-interface variables from large cliques using a combination of exact and approximate marginalization. The output is an approximate CTF, denoted CTF_a and a table IM containing links between cliques in CTF_{in} and CTF_a .

Algorithm 4 ApproximateCTF ($CTF_{in}, IV, mcs_{im}, E$)

Input: CTF_{in} : Input clique tree forest
 IV : Interface variables
 mcs_{im} : Maximum clique size limit for interface CTF
 E : Boolean variable indicating presence of evidence

Output: CTF_a : Approximate CTF
 IM : Dictionary linking cliques CTF_a to CTF_{in}

- 1: \triangleright Step 1: Identify the minimal subgraph connecting IV
- 2: $CTF_a \leftarrow$ Subgraph of CTF_{in} connecting IV
- 3: Prune CTF_a by recursively removing redundant leaf nodes
- 4: \triangleright Step 2: Collapse cliques and marginalize non-interface variables
- 5: $NIV \leftarrow Nets \in CTF_a \setminus IV$ \triangleright Non-interface variables
- 6: \triangleright Exact marginalization
- 7: Sum out NIVs present in a single clique in CTF_a
- 8: Remove resultant non-maximal cliques, reconnect neighbors;
- 9: $NI_m \leftarrow$ subset of NIV present in cliques with total size $< mcs_{im}$
- 10: Collapse cliques and marginalize out NI_m from CTF_a
- 11: \triangleright Step 3: Trim large cliques with size $> mcs_{im}$
- 12: $L_c \leftarrow$ List of cliques with size $> mcs_{im}$
- 13: Compute metrics maxMI, MLMI for interface and non-interface variables in all cliques in L_c
- 14: $N \leftarrow$ Non-interface variables present in cliques in L_c
- 15: **while** $L_c \neq \emptyset$ **do** $\triangleright CTF_a$ has cliques with size $> mcs_{im}$
- 16: **if** $N == \emptyset$ **then** $N \leftarrow$ interface variables present in cliques in L_c
- 17: $n = N$.pop net with the least maxMI
- 18: $L_{cn} \leftarrow$ List of cliques containing n .
- 19: $L_s \leftarrow$ Subset of L_{cn} with size $\leq mcs_{im}$
- 20: $L_r = \emptyset$ \triangleright List of cliques where n is retained
- 21: **if** $L_s \neq \emptyset$ **then** \triangleright There are cliques containing n with size $\leq mcs_{im}$
- 22: $L_{st} \leftarrow$ Disjoint subtrees in CTF_a over L_s
- 23: $L_r \leftarrow$ Subtree $\in L_{st}$ containing clique with largest MLMI
- 24: **else if** $n \in IV$ **then** \triangleright All cliques containing n have size $> mcs_{im}$
- 25: **if** E **then** **continue** \triangleright Ignore n to keep CT connected while inferring posteriors
- 26: **else** Add an independent clique C with $C = \{n\}$ \triangleright Do this if the CT can be disconnected
- 27: **end if**
- 28: MinSepSize \leftarrow Size of smallest sepset in subtree containing cliques in $L_{cn} \setminus L_r$
- 29: **if** $\neg E$ or $(E \& \& (\text{MinSepSize} > 1))$ **then**
- 30: Locally sum over states of n in all cliques in $L_{cn} \setminus L_r$ and corresponding sepsets
- 31: Remove resultant non-maximal cliques, reconnect neighbors
- 32: **end if**
- 33: $L_c.remove(C)$ if $C.size \leq mcs_{im} \ \forall C \in L_{cn} \setminus L_s$
- 34: **end while**
- 35: \triangleright Step 4: Create Interface Map: Map between cliques in CTF_a and CTF_{in}
- 36: $IM(C') =$ List of constituent cliques in $CTF_{in}, \ \forall C' \in CTF_a$ \triangleright Map between cliques in CTF_a and CTF_{in}
- 37: \triangleright Step 5: Re-assign clique factors
- 38: **for** $CT \in CTF_a$ **do**
- 39: root \leftarrow Pick a node at random from CT
- 40: $\psi_{root} = \beta_{root}; L_v = [root]$
- 41: **for** $C_i \in L_v$ **do**
- 42: **for** $C_j \in \{CT.neighbors(C_i) \notin L_v\}$ **do** $\psi_{C_j} = \beta_j / \mu_{ij}; L_v.add(C_j)$
- 43: **end for**
- 44: **end for**
- 45: **return** CTF_a, IM

The main steps in the algorithm are as follows.

Step 1: Identify the minimal sub-graph connecting interface variables: (lines 1-3 of Algorithm 4) We first identify the set of cliques that contain one or more interface variables and find the minimal subgraph of CTF_{in} that connects these cliques. This is done by identifying a subgraph that contains all these variables. Then, starting with the leaf nodes, cliques that contain the same set (or subset) of interface variables as their neighbor are removed recursively. The result is denoted CTF_a , which is used for approximation.

Step 2: Collapse cliques and sum out non-interface variables: (lines 4-10 of Algorithm 4) In this step, we attempt exact marginalization to remove nodes $n \in NIV$ from CTF_a . First (lines 7-8), the non-interface variables present in a single clique are identified, and the corresponding clique beliefs (β) are marginalized by summing over the states of these variables. If the resultant clique is a non-maximal clique, then it is removed from CTF_a , and its neighbors are connected to the containing clique. In case there are multiple containing cliques, we choose the one with the least number of neighbors for connection.

On the other hand (lines 9-10), if $n \in NIV$ is present in multiple cliques, we first identify a subtree ST_n containing n . The cliques in this subtree are collapsed into a single clique C_c , provided $\text{size}(C_c) \leq mcs_{im}$ and n is summed out. The belief corresponding to C_c is obtained as

$$\beta(C_c) = \sum_{n.\text{states}} \left(\frac{\prod_{C \in ST_n} \beta(C)}{\prod_{SP \in ST_n} \mu(SP)} \right), \quad SP \text{ denotes sepsets in } ST_n$$

CTF_a is obtained by connecting the branches of cliques that are collapsed to the new clique C_c . Figure 5a shows an example, where the cliques containing the non-interface node n_1 are collapsed. The branches are connected to the new clique as shown in Figure 5b.

At the end of this step, the joint distribution is preserved i.e., variables in CTF_a have the same joint distribution in CTF_a and CTF_{in} .

Step 3: Trim cliques with size $> mcs_{im}$: (lines 11-34 of Algorithm 4) The goal of this step is to bring down sizes of these cliques to mcs_{im} , while preserving the joint distribution of the interface variables as much as possible. The idea is to remove non-interface variables that are least correlated with the interface variables from a minimal set of cliques in CTF_a , with the following constraints.

- (a) Resulting CTF_a remains valid.
- (b) If there are evidence variables (E is TRUE), each connected $CT \in CTF_a$ remains connected. This is essential for computation of the partition function and posterior beliefs.

To do this, we define a metric based on pairwise mutual information (MI) between variables in a clique. Let IV_C and NIV_C denote the set of interface and non-interface variables in a clique C . For all variables in the clique, we define the *Maximum Local Mutual Information*, $MLMI$ as follows

$$MLMI_{n,C} = \begin{cases} \max_{\forall x \in IV_C} MI(n; x) & n \in NIV_C \\ \max_{\forall x \in C \setminus n} MI(n; x) & n \in IV_C \end{cases} \quad (1)$$

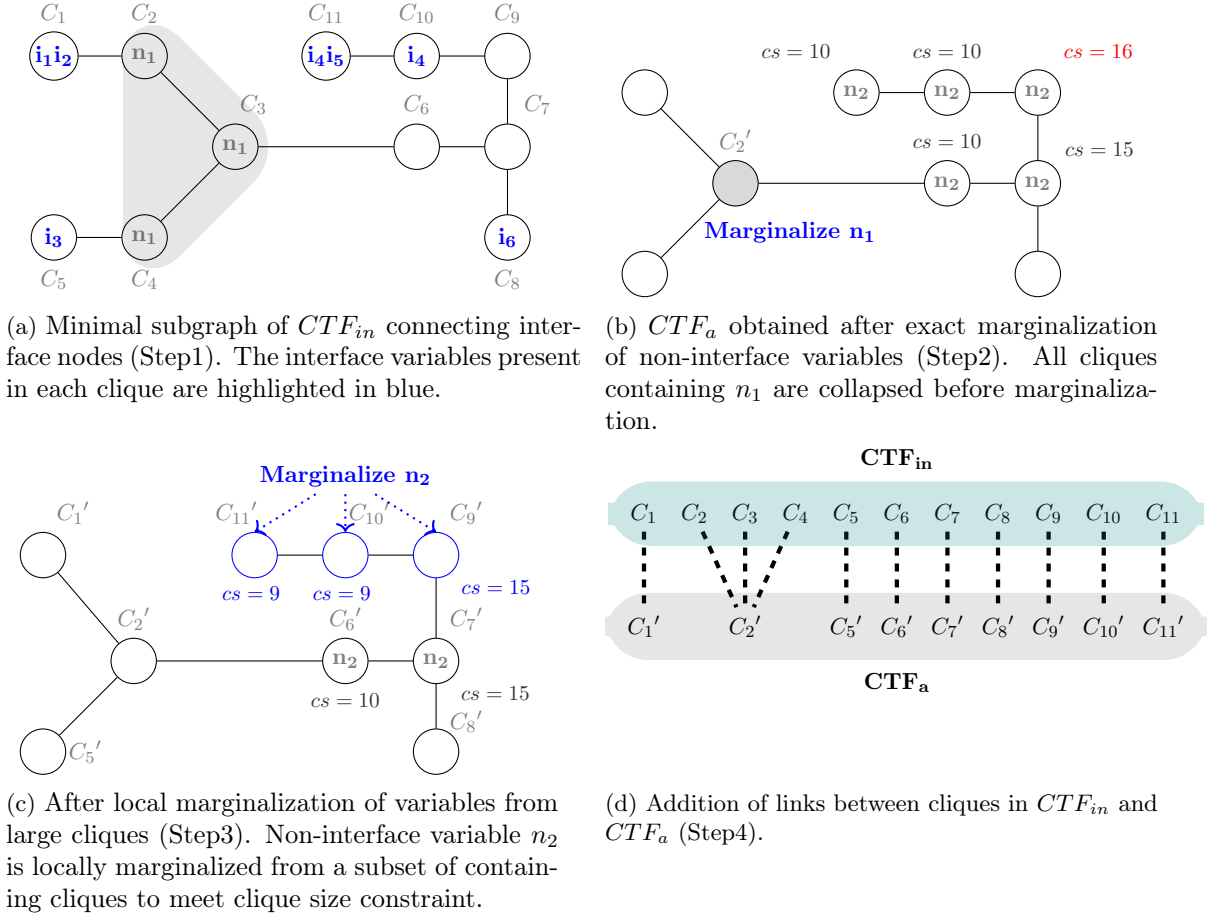


Figure 5: Illustration of the proposed approach to approximate the partition CTF. Each circle represents a clique. A subset of clique scopes is indicated inside each clique. While i_1, i_2, i_3, i_4, i_5 are interface variables, n_1, n_2 are non-interface variables.

where

$$MI(x; y) = \sum_{s \in D_x, w \in D_y} p(s, w) \log \frac{p(s, w)}{p(s)p(w)}$$

For a non-interface variables, $MLMI$ of a net is the maximum MI between the net and interface variables in the clique. $MLMI$ for an interface variables is defined as the maximum MI between the net and all the other variables in the clique.

The *Maximum Mutual Information*, $maxMI$ for both types of variables is defined as the maximum $MLMI$ over all cliques, given as

$$maxMI_n = \max_{\forall C \in CTF \text{ s.t. } n \in C} MLMI_{n,C} \quad (2)$$

CTF_a is first simplified by *locally marginalizing* out non-interface variables from individual large cliques while retaining them in as many smaller sized cliques consistent with RIP.

By local marginalization, we mean the following. Assume that a node n is present in two adjacent cliques C_i and C_j , and in the corresponding sepset $S_{i,j}$. Local marginalization results in two approximate cliques $C'_i = C_i \setminus n$ and $C'_j = C_j \setminus n$ with sepset $S'_{i,j} = S_{i,j} \setminus n$. The corresponding beliefs are

$$\beta(C'_i) = \sum_{n.states} \beta(C_i), \quad \beta(C'_j) = \sum_{n.states} \beta(C_j), \quad \mu(S'_{i,j}) = \sum_{n.states} \mu(S_{i,j})$$

The nets chosen for local marginalization are ones with the least $maxMI$, since these nets have the lowest MI with the interface variables.

The steps involved in performing local marginalization are as follows. The line numbers in the following description correspond to those in Algorithm 4. We first identify the set of large cliques with size $> mcs_{im}$ and store them in a list L_c (line 12). The metrics $maxMI$, $MLMI$ are computed for all variables in L_c (line 13). Then, we find the set of non-interface variables present in these cliques and add them to a list N (line 14). We start with the node n that has the least $maxMI$. In order to retain n in as many cliques as possible, we find the list of cliques containing n with size $\leq mcs_{im}$ and store them in a list L_s (lines 18-19). Next, we identify the subgraph of CTF_a corresponding to cliques in L_s and divide it into a set of disjoint subtrees, L_{st} (line 22). Net n is retained in the subtree that contains the clique with largest $MLMI$, denoted as L_r (line 23). In case of a tie, we choose the subtree with the largest number of cliques. Net n is locally marginalized out from all other containing cliques and sepsets, while ensuring each connected CT remains connected if evidence is present (lines 29-31). Any resultant non-maximal clique is removed, and its neighbors are connected to the containing clique.

Figure 5c shows an example of this step. The non-interface net n_2 is locally marginalized out from three of the cliques, while it is retained in the other two cliques.

Once this is done, if there are cliques with size $> mcs_{im}$, they will contain only interface variables and non-interface variables that cannot be removed without breaking a connected CT. The interface variables are added to the list N (line 16) and following the same procedure as for NIVs, the interface variable is retained in the subtree that contains the clique with largest $MLMI$.

However, there is one difference (lines 25-27). An interface variable must be contained in at least one clique in CTF_a . If there are no cliques with size $\leq mcs_{im}$ containing a particular interface variable and E is TRUE (indicating evidence is present), the algorithm proceeds to the next variable without doing anything. This is because we require a connected CT to remain connected. In some applications, for example in circuits, only the prior probabilities are needed. In these cases, the CT can be split and we can create an independent node with just the interface variable (line 26).

Step 4: Create Interface Map (IM) (lines 35-36 of Algorithm 4) For each clique $C' \in CTF_a$, we add a link to a clique or a set of cliques in CTF_{in} as follows

- If C' is obtained after collapsing a set of cliques $\{C_1, \dots, C_m\} \in CTF_{in}$, links is added from C' to each of $\{C_1, \dots, C_m\}$.
- If C' is obtained from $C \in CTF_{in}$ after a local marginalization, a link is added from C' to C .

- If C' is same as clique $C \in CTF_{in}$, a link is added from C' to C .

IM is implemented as a Python dictionary, with cliques in $C' \in CTF_a$ used as keys and the corresponding cliques in CTF_{in} as values.

Figure 5d shows the links between CTF_{in} and CTF_a for the example. The collapsed clique C_2' gets linked to the constituent cliques C_2, C_3, C_4 .

Step 5: Re-assignment of clique factors: (lines 37-44 of Algorithm 4) For each CT in the CTF_a , a root node is chosen at random. The factor for the root node is the same as the clique belief (lines 40). All other nodes are assigned factors by iterating through them in pre-order, i.e., from the root node to leaves. An unvisited neighbor C_j' of a node $C_i' \in CTF_a$ is assigned the conditional belief $\beta(C_j'|C_i') = \frac{\beta(C_j')}{\mu(S'_{i,j})}$ as a factor.

5.1 Properties of the approximated CTF

In the following, we use the terms CTF_{in} and CTF_a to denote the input and output CTF of Algorithm 4. The two CTFs satisfy the following properties. The line numbers indicated in the various propositions refer to line numbers of Algorithm 4.

Proposition 5. *If all CTs in CTF_{in} are valid, then all CTs in CTF_a are valid.*

Proof. CTF_a obtained after the first step is valid since it is a subgraph of the CTF_{in} that connects the cliques containing variables in IV . The CTs in CTF_a obtained after the subsequent steps are valid because of the following reasons.

- It contains only maximal cliques. Any non-maximal cliques generated while simplification of CTF_a are removed. (lines 8, 31).
- It contains disjoint trees.
In Step 2, neighbors of the collapsed and non-maximal cliques are reconnected to CTF_a such that connectivity of the CTs is preserved. In Step 3, If the BN has evidence variables, non-interface variables are removed only if no sepset size becomes zero, ensuring that a connected CT remains connected. (lines 29-31). If the BN has no evidence variables, then a connected CT could break up into disjoint trees (line 26). In either case, no loops are introduced.
- It satisfies RIP.
 - In Step 2, sepsets in the CTF_a are preserved while re-connecting the neighbors of the collapsed cliques to the new clique, thereby ensuring that RIP is satisfied. Similarly, since neighbors of non-maximal cliques which are removed are connected to the containing cliques, sepsets are preserved.
 - In Step 3, variables are retained in a single connected component of CTF_a (lines 21-23). Therefore, the subgraph of CTF_a over any net is connected.
- The re-assignment of factors in Step 5 results in a valid distribution
After collapse and exact marginalization, all the clique and sepset beliefs are preserved. Therefore, the resultant clique is also calibrated. Let C_i and C_j be two adjacent

cliques in CTF_{in} with sepset $S_{i,j}$. After local marginalization of a node n , we get the corresponding cliques $C'_i, C'_j \in CTF_a$, with sepset $S'_{i,j}$. Since the result is invariant with respect to the order in which variables are summed out, we have

$$\sum_{C'_i \setminus S_{i,j}'} \beta(C'_i) = \sum_{C'_i \setminus S_{i,j}'} \sum_{n.states} \beta(C_i) = \sum_{n.states} \sum_{C'_i \setminus S_{i,j}'} \beta(C_i) = \sum_{n.states} \mu(S_{i,j}) = \mu(S'_{i,j})$$

where we use $n.states$ to denote the states of n . Similarly $\sum_{C'_j \setminus S_{i,j}'} \beta(C'_j) = \mu(S'_{i,j})$. Since this is true for pair of adjacent cliques, CTF_a is calibrated. In Step 5, the re-assignment of factors is done using the calibrated CTF beliefs. Therefore, the product is a valid distribution. \square

Recall that for BNs with evidence, the BP algorithm uses the un-normalized clique beliefs. Exact inference on a CT uses two rounds of message passing, after which the *normalization constant* of all clique and sepset beliefs are the same and are equal to the partition function (Koller & Friedman, 2009). In our algorithm, the DAGs are simplified and the CTF is constructed incrementally for each DAG. Evidence variables could be added in any of the partitions. We also use un-normalized clique beliefs and the standard BP algorithm (Koller & Friedman, 2009) for each partition. The following proposition holds for our algorithm.

Proposition 6. *Algorithm 4 preserves the normalization constant and the within-clique beliefs of all cliques in CTF_a .*

Proof. CTF_a is obtained from CTF_{in} , which is calibrated. If there is no evidence, the clique beliefs in CTF_{in} are the joint probability distribution of the variables in the clique. In the presence of evidence, the clique beliefs are un-normalized and all cliques in a CT have the same normalization constant.

After exact marginalization (lines 4-10), the clique beliefs in CTF_a are identical to the beliefs in CTF_{in} , since the step involves collapsing all containing cliques before marginalization of beliefs. Marginalization does not change the normalization constant. In the approximation step (lines 11-34), some variables are locally marginalized out from individual cliques by summing over the states of those variables. Summing over the states of a variable does not change either the beliefs or the normalization constant of the remaining variables. The factors are also assigned so that within-clique beliefs are preserved. \square

Note that the joint beliefs of variables present in different cliques of a CT in CTF_a may not be preserved. This is because variables that are locally marginalized from a clique are also locally marginalized from the corresponding sepsets.

Proposition 7. *If the clique beliefs are uniform, then the beliefs obtained after approximate marginalization is exact*

Proof. Let C_1 and C_2 be two adjacent cliques in CTF_{in} with sepset $S_{1,2}$. After local marginalization of a node n , we get the corresponding cliques $C'_1, C'_2 \in CTF_a$, with sepset

$S'_{1,2}$. Let b_1 , b_2 and b_3 represent the uniform beliefs in C_1 , C_2 and $S_{1,2}$. If the node n has k states, the beliefs of states in C'_1 , C'_2 and $S'_{1,2}$ are kb_1 , kb_2 and kb_3

The exact joint belief of C_1 and C_2 is

$$\beta(C_1 \cup C_2) = \frac{\beta(C_1)\beta(C_2)}{\mu(S_{1,2})}$$

Each state of $\beta(C_1 \cup C_2)$ has a constant belief $\frac{b_1 b_2}{b_3}$. With exact marginalization, the states of $\sum_{n.states} \beta(C_1 \cup C_2)$ have a constant belief $k \frac{b_1 b_2}{b_3}$. With local marginalization, the joint beliefs are

$$\beta(C'_1 \cup C'_2) = \frac{\beta(C'_1)\beta(C'_2)}{\mu(S'_{1,2})}$$

The corresponding constant beliefs are $\frac{(kb_1)(kb_2)}{kb_3} = k \frac{b_1 b_2}{b_3}$. □

6. Inference of Marginals and the Partition function

We first summarize the notations relevant to this section. Let CTF_i denote the CTF for the i^{th} DAG in the BN. The n_i partitions of the i^{th} DAG are denoted $\{Q_{i1}, Q_{i2}, \dots, Q_{in_i}\}$, with corresponding CTFs $CTF_i = \{CTF_{i,1}, CTF_{i,2}, \dots, CTF_{i,n_i}\}$. $CTF'_{i,k}$ denotes the approximate CTF corresponding to $CTF_{i,k}$, obtained using Algorithm 4. The cliques of $CTF'_{i,k}$ are the keys in the dictionary $IM_{i,k}$, which contains links to corresponding cliques in $CTF_{i,k}$. The variables in $CTF'_{i,k}$ are denoted **link variables**. These variables are present in both $CTF_{i,k}$ and $CTF_{i,k+1}$.

6.1 Prior marginals (MAR_p)

Once the iteration in Algorithm 1 concludes (line 31), the CTFs for each DAG in the BN and the corresponding calibrated beliefs for each partition are available in L_{CTF} . In the absence of evidence, the prior marginals of all variables can be inferred from these beliefs, using the following proposition.

Proposition 8. *In the absence of evidence, the prior singleton marginals can be obtained from any partition in which it is present.*

Proof. From Proposition 6, we know that the within-clique beliefs of all cliques are preserved by Algorithm 4. $CTF'_{i,k}$ is constructed by adding new nodes to $CTF'_{i,k-1}$. These new nodes are successors of nodes present in $CTF'_{i,k-1}$. Since there are no evidence variables, addition of these nodes will not affect beliefs of nodes already present in $CTF'_{i,k-1}$. Since this is true for all partitions, the prior beliefs of nodes are consistent across partitions and can be obtained from any partition. □

6.2 Partition function and Posterior Marginals (PR , MAR_e)

As discussed in section 3, after simplification of the BN, we get a set of disjoint DAGs. If exact inference is used, corresponding to each DAG, we will get a single CT and the normalization constant of the CT is the probability of the evidence variables present in the DAG. The partition function is the product of the normalization constants of CTs

corresponding to each DAG. In our method, we build the CT for a DAG incrementally, starting from a CTF containing disjoint nodes. As more and more nodes are added, the CTs get connected. If evidence is present, Algorithm 4 (lines 25, 29) ensures that a connected CT always remains connected, which means that for each DAG, the last partition has a single connected CT. In this section, we discuss the algorithm used to find PR and MAR_e , given the calibrated CTFs of all partitions. As mentioned, un-normalized clique beliefs are obtained after calibration.

Based on the properties of Algorithm 4, we have the following.

Proposition 9. *The normalization constant of a $CT \in CTF_{i,k}$ is the estimate of probability of all evidence states added to it in the current and all preceding partitions $Q_{ij}, j \leq k$.*

Proof. Inference is exact for the first partition. Therefore, after calibration, the normalization constant of each CT for the first partition is the probability of evidence states added to the CT. Using Proposition 6, we know that the normalization constant of CTs in $CTF'_{i,k-1}$ is same as the normalization constant of CTs in $CTF_{i,k-1}$. Therefore, $CTF'_{i,k-1}$ takes into account all evidence states added upto partition $k - 1$. $CTF_{i,k}$ is constructed by adding new nodes to $CTF'_{i,k-1}$. We first consider the case where a CT in $CTF_{i,k}$ is obtained from a single CT in $CTF'_{i,k-1}$. After adding as many nodes as possible, the CT is calibrated. Therefore, after calibration, updated normalization constant will account for the evidence present in $CTF_{i,k-1}$ as well as any new evidence variables added to the CT.

The second case occurs when multiple CTs in $CTF'_{i,k-1}$ get connected to form a single CT in $CTF_{i,k}$. Using the same argument, after calibration of this new CT using BP, its normalization constant will reflect the probability of evidence present in all the constituent CTs as well as the new evidence variables added.

The proposition follows since this is true for all partitions. \square

Theorem 2. *The product of the normalization constants of the CTs corresponding to the last partition of all DAGs is the estimate of Partition Function (PR).*

Proof. For each DAG, G_i , the last partition CTF contains a single CT, since we never break a connected CT. Using Proposition 9, the normalization constant (PR_i) for this CT is the estimate of the probability of evidence variables present in G_i . This value is exact when there is only one partition and may be approximate when there are multiple partitions. The product $\prod_i PR_i$ is the estimate of the overall partition function PR of the BN. \square

Based on Theorem 2, Algorithm 5 computes the partition function.

Algorithm 5 ComputePF(L_{CTF})

```

1:  $PR = 1$ 
2: while  $L_{CTF}$  is not empty do
3:    $CTF = L_{CTF}.pop$ 
4:    $CTF_l = CTF[-1]$ 
5:    $C \leftarrow$  Choose any clique in  $CTF_l$ 
6:    $PR = PR \times \sum_{v \in C} \sum_{s \in v.states} \beta_C$ 
7: end while
8: return  $PR$ 
```

\triangleright Pop a list of CTFs corresponding to a DAG
 \triangleright Get the CTF corresponding to the last partition
 \triangleright Sum over all beliefs in the clique

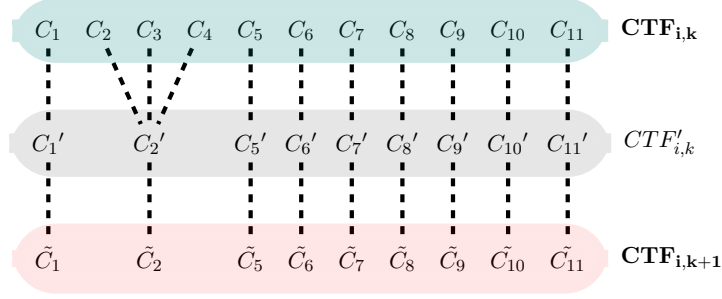


Figure 6: Links connecting $CTF_{i,k+1}$ to $CTF_{i,k}$ via the approximate CTF of the previous partition.

6.2.1 COMPUTATION OF POSTERIOR MARGINALS

For the i^{th} DAG, let Q_{ie_i} be the last partition to which new evidence variables are added. These partition numbers are contained in the list LQ_e (See line 25 in Algorithm 1). The following result follows

Theorem 3. *The singleton posterior marginals of variables in partitions $\{Q_{ij}, j \geq e_i\}$ is preserved and can be computed from any of these partitions.*

Proof. Based on Proposition 6, we know that within-clique beliefs are preserved after approximation. Additional nodes added in each new partition can only contain successors. Therefore, if no new evidence variables are added, the beliefs of the previous nets remain unchanged. Thus, the singleton posterior marginals of variables in partitions $\{Q_{ij}, j \geq e_i\}$ will be preserved and can be computed from any of these partitions. \square

Based on Theorem 3, we can get the posterior marginals of all variables in partitions $\{Q_{ij}, j \geq e_i\}$. However, the CTs in partitions $\{Q_{ij}, j < e_i\}$ need to be updated for evidence states introduced in later partitions. To do this we propose a heuristic back propagation algorithm for belief update, that successively updates beliefs in $Q_{i,k}$ so that it is consistent with the subsequent partition $Q_{i,k+1}$, starting from $k = e_i - 1$. Effort for re-calibration increases with e_i . Therefore, we prioritize addition of evidence variables while construction of CTs so that they are added as early as possible (line 20, Algorithm 3). Following are the detailed steps for backpropagation.

Step 1: Update interface map:

The CTF for the next partition $CTF_{i,k+1}$ is built using $CTF'_{i,k}$ as the starting point. While building $CTF_{i,k+1}$, the cliques $C'_j \in CTF'_{i,k}$ could morph into new cliques \tilde{C}_j . In this step, for each C'_j in the dictionary $IM_{i,k}$, an additional clique, $\tilde{C}_j \in CTF_{i,k+1}$, s.t. $C'_j \subset \tilde{C}_j$, is added. At the end of this step, each C'_j in $IM_{i,k}$ has links to one or more cliques in the preceding partition and a link to a clique in the subsequent partition. Figure 6 shows links between $CTF_{i,k}$ and $CTF_{i,k+1}$ via $CTF'_{i,k}$. Algorithm 6 describes the procedure used.

Step 2: Back propagation of beliefs

If new evidence variables are added to $CTF_{i,k+1}$, the beliefs of $\tilde{C}_j \in CTF_{i,k+1}$ will become

Algorithm 6 FindInterfaceLinks(LQ_e, L_{CTF}, L_{IL})

Input: LQ_e : List containing the last partition to which evidence variables are added for each DAG

L_{CTF} : List of CTFs for each DAG in the BN

L_{IL} : List of interface maps for each partition of a CTF

```
1: for  $i = 1$  to  $\text{len}(LQ_e)$  do
2:    $e_i = LQ_e[i]$ 
3:   if  $e_i == 1$  then continue
4:    $L = L_{CTF}[i]; M = L_{IL}[i]$ 
5:   for  $k = 1$  to  $e_i - 1$  do
6:      $CTF_{i,k+1} = L[k+1]; IM_{i,k} = M[k];$ 
7:      $\triangleright IM$  is a dictionary with approximate cliques as keys
8:      $C_a = IM_{i,k}.\text{keys}()$ 
9:      $\triangleright$  Add links between approximate cliques of partition  $Q_{ik}$  and cliques in the  $CTF_{i,k+1}$ 
10:     $IM_{i,k}(C_j').\text{add}(\tilde{C}_j), \forall C_j' \in C_a \text{ such that } C_j' \subseteq \tilde{C}_j \in CTF_{i,k+1}$ 
11:  end for
12: end for
```

consistent with the new evidence. The beliefs of a corresponding clique $C_j \in CTF_{i,k}$ are updated via the link C_j' as follows:

$$\beta(C_j) = \frac{\beta(C_j)}{\beta(C_j')} \sum_{\tilde{C}_j \setminus C_j'} \beta_{\tilde{C}_j} \quad (3)$$

This is followed by one round of message passing from C_j to all other cliques in the CT containing C_j . After this step, the beliefs in $CTF_{i,k}$ agree with the beliefs in $CTF_{i,k+1}$ only over variables present in that particular link. Belief update of other variables is approximate.

There are multiple links via which the beliefs $CTF_{i,k}$ can be updated. To ensure that every $CT \in CTF_{i,k}$ is re-calibrated, at least one link must be chosen for each CT. It is also clear that more than one link may be required since variables that have low correlations in $CTF_{i,k}$ could become tightly correlated in $CTF_{i,k+1}$ (due to the additional evidence in $Q_{i,k+1}$, for example). Empirically, we have found that updating via all links gives the best result. But it is expensive since each update via a link requires a round of message passing in $CTF_{i,k}$. Based on results over many benchmarks, we use the following heuristics to choose and schedule links for backward belief update.

1. We first find the difference in the normalized marginals of all the link variables in both $CTF_{i,k}$ and $CTF_{i,k+1}$. Link variables for which this difference is less than a threshold are discarded. For each remaining link variable, we find the containing clique $C_j \in CTF_{i,k}$ with the maximum number of link variables. The minimum set of cliques covering these remaining link variables is chosen for belief update.
2. The updated beliefs depend on the order in which the links are used for update. Based on the difference in marginals, we form a priority queue with the cliques containing link variables that have the lowest change in marginals having the highest priority. This is to make sure that large belief updates do not get over-written by smaller ones. This could happen for example, if two variables (say, v_1, v_2) that are highly correlated in partition k become relatively uncorrelated in partition $k+1$ due to the approximation. If the evidence added to partition $k+1$ affects v_1 but not v_2 , backpropagation through link containing v_1 ensures that both v_1 and v_2 are modified in accordance to the new evidence. However, this could be overwritten if backpropagation through v_2 is performed after v_1 .

Algorithm 7 describes the steps.

Note: The posterior marginals of variables obtained after back-propagation are *not* the same in all partitions in which they are present. They are inferred in the first partition in which they are introduced. This is to make sure that they are inferred after all their successors have been updated (line 19 of Algorithm 7).

Algorithm 7 GetPosterior(L_{CTF} , L_{IL} , LQ_e)

Input: L_{CTF} : List of CTF for each partition
 L_{IL} : List of interface link maps
 LQ_e : List containing the last partition to which new evidence variables for each DAG

Output: MAR : Posterior marginals

```

1:  $N_d = \text{len}(L_{CTF})$  ▷ Number of DAGs in BN
2: FindInterfaceLinks( $LQ_e$ ,  $L_{CTF}$ ,  $L_{IL}$ )
3: for  $i = 1$  to  $N_d$  do ▷ Iterate over all DAGs in the BN
4:    $e_i \leftarrow LQ_e[i]$  ▷ First partition with single CT and all evidence variables in the  $i^{th}$  DAG
5:    $L \leftarrow L_{CTF}[i]$ 
6:    $M \leftarrow L_{IL}[i]$ 
7:   for  $k \geq e_i$  do  $MAR[v] \leftarrow$  Infer marginals of variables in these partitions using any containing clique
8:   for  $k \in e_i - 1$  down to  $1$  do
9:      $IM_{i,k} \leftarrow M[k]$  ▷ Get link table for the partition
10:     $CTF_{i,k} \leftarrow L[k]$ ;  $CTF_{i,k+1} = L[k+1]$ 
11:     $L_l \leftarrow$  Ordered list of links in  $IM_{i,k}$  selected using heuristics in section 6.2.1
12:    ▷ Backpropagate via all selected links
13:    for  $(C, C', \tilde{C}) \in L_l$  do
14:      Update  $\beta(C) \in CTF_{i,k}$  based on  $\beta(\tilde{C}) \in CTF_{i,k+1}$  over common variables in  $C'$  using Equation 3
15:      Update belief of all other cliques in  $CTF_{i,k}$  using single pass message passing with  $C$  as the root node
16:    end for
17:  end for
18:  ▷ Infer marginals
19:   $MAR[v] \leftarrow$  Find marginal from  $CTF_i$  s.t.  $v \in Q_j, v \notin Q_{j-1} \quad \forall v \in \{Q_1, \dots, Q_{e_i} - 1\}$ 
20: end for
21: return  $MAR$ 

```

7. Complexity, trade-offs and comparison with related work

7.1 Complexity

Let L be the number of topological levels in the BN and P be the number of partitions generated by our algorithm. For each partition, we perform three main steps. We now discuss the worst-case complexity of each of these steps.

1. Build CTF: In each iteration, we add active nets at a particular topological level. A new clique is added to the CT for nets belonging to Cases 1 and 2 in Algorithm 3, which is an $O(1)$ operation. Nets \in Case 3 of Algorithm 3 are grouped into subsets that affect overlapping portions of the CT. All nodes in a subset are added together. The complexity of addition depends on the number of subgraphs and the cost of re-triangulating each subgraph. In the worst case, the subgraphs are as large as the CTs $\in CTF$ for every set of nodes added, and there are no retained cliques. The cost of re-triangulation ($Cost_R$) is polynomial in the number of variables in CTF (Koller & Friedman, 2009). Hence, the worst-case complexity is upper bounded by $O(P \cdot L \cdot Cost_R)$. Generally, the number of computations required is much lower since there are many retained cliques and different subsets impact disjoint subgraphs of the

existing CTs. There is also considerable scope for parallelism here since each impacted subgraph can be processed independently.

2. Inference and Approximation: Since we use exact inference to calibrate the clique-tree, the complexity of inference in each partition is $O(2^{mcs_p})$. Approximation involves summing out variables from a belief table. Once again, this is $O(2^{mcs_p})$. The overall complexity is therefore $O(P \cdot 2^{mcs_p})$.
3. Complexity of belief update via back-propagation: Each belief update involves belief update of a single clique via the link, followed by one round of message passing to re-calibrate the clique tree. Let N_l is the maximum number of links between adjacent partitions. In the worst case, we backpropagate beliefs from the last to the first partition via N_l links. Therefore, the worst-case complexity is $O(P \cdot N_l \cdot 2^{mcs_p})$.

7.2 Comparison with related work on partitioning and approximate inference

We compare our algorithm with existing methods in terms of (a) Methods to obtain bounded cluster sizes (b) trade-off between accuracy and complexity and (c) Consistency of beliefs after approximation.

In methods proposed in the literature, the process of partitioning to get bounded cluster sizes follows two routes. One is a straightforward scope or structure-based partitioning used in mini-bucket elimination and some region graph based methods. The second technique is an iterative process that involves multiple rounds of structure/region reconstruction and approximate belief propagation, until “good” regions are identified. Either approximate factorized messages are used or exact BP algorithms are run on relaxed structures or local message passing/relative entropy computations are used to get approximate beliefs. Our method partitions the network in an entirely different way. Unlike all other methods, we focus on the clique trees in our method, constructing them incrementally. Our method simply keeps adding nodes to the clique tree until the bound is reached. We do not explicitly try to identify “good regions” or nodes for duplication. Instead, once we reach the maximum permissible clique size, we calibrate the CT using the standard two-pass BP algorithm and use calibrated beliefs for approximation. We do not need to use iterative belief propagation, which may or may not converge.

A big advantage of our method is the ease of approximating a clique tree for use as the starting point for the next partition, in a way that consistency conditions are satisfied. Since we always marginalize beliefs by summing out variables, the approximation preserves within-clique beliefs. In the absence of evidence, this automatically ensures consistency of singleton marginals. Marginal consistency is ensured via edge parameters in Choi and Darwiche (2006). In our algorithm, not only the singleton beliefs but the beliefs of all link variables present in a clique are consistent across partitions once all evidence variables are added to the CT (see Proposition 8 and Theorem 3).

Our method can also be viewed as partitioning with clique duplication (instead of node duplication). However, instead of deleting edges we reduce the size of the clique by summing out some of the variables that do not have successors that have not been added to the clique tree.

The other consistency condition in Choi and Darwiche (2006) is to take care of “lost evidence”. They fix this by adding auxiliary evidence nodes, whose posterior marginal is specified in terms of posterior beliefs of evidence, given the clone node. We do this in a different way. In our algorithm, “lost evidence” for a partition would be the evidence variables added in subsequent partitions. We do not add auxiliary evidence nodes. Rather, we update beliefs via back propagation. However, we do use inferred marginals in adjacent partitions to guide the choice and sequence of links via which this updating is done. Our belief update method, however is heuristic and approximate. We do not have consistency of posterior marginals across partitions for all variables. The posterior beliefs are inferred in the first partition in which the variable is added, in order to make sure it is inferred after its successors are updated.

Like some of the other methods, we can trade-off time and space complexity for accuracy. Many of the factor based clustering techniques to improve accuracy require multiple rounds of belief propagation and region reconstruction. The number of such iterations performed controls the accuracy of the method. In IJGP and WMB, the trade-off is based on a single parameter making it very convenient. Like IJGP and WMB, the trade-off is easy to achieve in IBIA, since we have only two parameters. Moreover, in our algorithm, we use a combination of size and factor based partitioning. Clique sizes are limited to mcs_p within a partition and factor based information is used to reduce the size of the cliques to mcs_{im} during approximation. The reduction in clique sizes is done after exact join-tree based inference, but *within a partition containing bounded clique sizes*. Higher values of mcs_p results in better accuracies, but increased complexity of exact inference in each partition due to larger clique sizes. mcs_{im} controls the amount of approximation. Lower values of mcs_{im} implies more aggressive approximations, but generally, a smaller number of partitions. It is not used as a hard constraint in our algorithm. We try to bring down the clique sizes to mcs_{im} , but allow for higher values when it is not possible. Lower or high values can also be used depending on domain sizes of variables.

An early method to partition the BN into multiple sections is the multiply section Bayesian network (MSBN) method proposed in Xiang et al. (1993). The focus of MSBN is exact inference with multiple sections connected via links. Co-operative triangulation of adjacent sections is used to get consistency (Xiang & Lesser, 2003). A requirement for this method is “sound sectioning”, that is, there are no cycles in the graph connecting sections. However, this algorithm does not guarantee bounds on clique sizes within a section. Finding partitions with bounded clique sizes just based on the structure of the BN would involve repeated re-triangulations of a large number of candidate sections, which is computationally infeasible. We overcome this by building the CTs incrementally. As in MSBN, we have links between partitions, that can be used for belief update. In our case, the links are the cliques in the approximated CT. In MSBN, the links are cliques obtained using co-operative triangulation.

7.3 Comparison with related work on incremental construction of CTs

To construct CTs with bounded clique sizes, we need an incremental approach to add variables to an existing CT model. An incremental modification approach using the Maximal Prime Subgraph Decomposition (MPD) of the BN is discussed in Flores et al. (2002). In

this method, based on the moralized graph, the CT is converted into another graphical representation called the MPD join tree. The minimal subgraph of the moralized graph that needs re-triangulation is identified using the MPD tree. This subgraph is re-triangulated, and both the CT and MPD join trees are updated. In contrast, our method,

- Requires lesser effort for re-triangulation. This is because the minimal subgraph that is re-triangulated is a portion of the modified chordal graph corresponding to the CT instead of the moralized graph. Moreover, as opposed to Flores et al. (2002), the subgraph identified using our method need not always contain all variables present in the scope of impacted cliques in CT.
- Eliminates the memory and runtime requirements for maintaining additional representations like the moralized graph, MPD join tree. Our method identifies the minimal subgraph to be re-triangulated directly from the CT, triangulates it and updates the CT. No other representation of the BN is needed.

8. Results

8.1 Evaluation of Algorithms in IBIA

We first evaluate IBIA with respect to the performance of the incremental CT construction algorithm and accuracy-runtime trade-off. Exact solutions were obtained using ACE (Chavira & Darwiche, 2008). The error metrics used in this evaluation are the modulus of the maximum error in the probability over all states of all non-evidence variables (max-error) and root mean squared error (RMSE) for MAR_e and MAR_p and $\log PR_{ACE} - \log PR_{IBIA}$ for PR. Solutions are tabulated for a subset of benchmarks, but the results for other benchmarks are similar.

8.1.1 EVALUATION OF INCREMENTAL CT CONSTRUCTION

We used the following method to evaluate our method for incremental construction of the CT. For a given mcs_p , we used Algorithm 3 to construct the CTF for the first partition incrementally. For comparison, we used a CTF obtained using full compilation of all the nets in the partition. This is done as follows. We first identified the subgraph of BN over all variables in CTF for the first partition and compiled the entire subgraph using variable elimination (Koller & Friedman, 2009). The elimination order is found using the ‘min-fill’ metric, and the metric ‘min-neighbors’ is used in case of a tie (Koller & Friedman, 2009). Re-computing the number of fill-in edges each time a variable is eliminated increases the execution time. Therefore, we adopted the methodology suggested in Kask et al. (2011) to compute only the change in the number of fill-in edges. The input BN was used without any evidence-based simplifications.

Table 1 compares the maximum clique size (refer Equation 10 for definition) obtained using incremental (mcs_i) and full compilation (mcs_f), for various values of mcs_p for a subset of benchmarks. The results for others are similar. We limited mcs_p to 25, since memory constraints in our system do not allow inference beyond this size. In general, we find that the difference, $mcs_i - mcs_f$, grows as mcs_p increases, which is to be expected. However, as long as mcs_p is limited to about 25, the difference is ≤ 2 in most cases. Even for testcases

like blockmap_15_01-0006 where the partition size is 5000, the clique sizes obtained using our method are within ± 1 of the size obtained using full recompilation. An exception to this is the Grid-BN benchmarks, where we find that the difference increases more rapidly. This is because these networks have a localized structure that enforces a particular elimination order when the incremental method is used.

Table 1: Comparison of the maximum clique size obtained after incremental construction (mcs_i) of the first partition with that obtained after full compilation of the corresponding BN subgraph (mcs_f). For each benchmark, we show results for partitions obtained using different clique size constraints. Entries are marked with ‘-’ if $mcs_p < \text{maximum CPD size}$. $\Delta = mcs_i - mcs_f$.

Network	$mcs_p = 10$				$mcs_p = 15$				$mcs_p = 20$				$mcs_p = 25$			
	#Nodes	mcs_i	mcs_f	Δ	#Nodes	mcs_i	mcs_f	Δ	#Nodes	mcs_i	mcs_f	Δ	#Nodes	mcs_i	mcs_f	Δ
BN_21	-	-	-	-	624	13.2	15.2	-1.9	627	17.2	16.2	1	2832	20.2	21.2	-1
BN_49	183	10	10	0	350	14	14	0	461	20	19	1	540	25	25	0
BN_60	201	10	10	0	257	15	14	1	323	20	18	2	341	25	25	0
BN_62	173	10	10	0	343	14	14	0	455	20	19	1	517	24	23	1
BN_66	101	8	8	0	157	15	15	0	196	18	17	1	242	25	25	0
BN_51	183	10	10	0	357	15	15	0	467	20	19	1	541	25	25	0
BN_55	217	10	10	0	254	15	15	0	294	20	20	0	309	25	23	2
mastermind_03_08_03-0010	376	10	11	-1	579	15	16	-1	743	20	20	0	817	22	19	3
mastermind_03_08_04-0010	372	10	10	0	748	15	15	0	1051	20	21	-1	1204	25	24	1
mastermind_03_08_05-0010	339	6	6	0	591	15	15	0	1135	18	18	0	1503	25	24	1
mastermind_04_08_03-0010	425	10	11	-1	632	15	16	-1	796	20	21	-1	997	25	25	0
mastermind_04_08_04-0010	568	10	10	0	758	15	16	-1	1080	20	20	0	1371	25	28	-3
mastermind_05_08_03-0010	495	10	11	-1	630	15	16	-1	837	20	20	0	1045	25	30	-5
mastermind_06_08_03-0010	555	10	11	-1	728	15	16	-1	893	20	22	-2	1111	25	25	0
mastermind_10_08_03-0010	773	10	11	-1	941	15	18	-3	1117	20	20	0	1323	25	27	-2
blockmap_10_01-0005	477	10	10	0	1076	15	16	-1	1602	20	20	0	2165	25	24	1
blockmap_15_01-0006	1177	10	11	-1	1873	15	15	0	3851	20	21	-1	5001	25	24	1
blockmap_10_02-0008	180	10	11	-1	318	15	15	0	382	19	19	0	590	25	25	0
90-42-5	292	10	10	0	399	15	13	2	531	20	16	4	583	25	18	7
90-23-5	171	10	10	0	206	15	12	3	235	20	14	6	268	24	15	9
50-18-5	131	10	10	0	194	15	13	2	229	20	18	2	251	24	22	2
75-25-5	190	10	9	1	209	13	11	2	252	20	18	2	276	25	20	5
90-50-5	517	10	9	1	598	15	13	2	740	20	18	2	848	25	19	6
andes	147	10	8	2	206	15	13	2	212	20	15	5	219	24	18	6
munin1	68	9.2	9.2	0	74	13.3	13.3	0	80	17.6	17.6	0	129	24	25	-1
munin4	283	9.6	9.6	0	301	13.9	14.2	-0.3	634	19.6	21.4	-1.8	642	20.4	21.4	-1
diabetes	-	-	-	-	186	13.6	13.6	0	192	19.2	18.9	0.4	196	22.7	18.2	4.5

8.1.2 IMPACT OF mcs_p AND mcs_{im} ON ERROR AND RUNTIME

As discussed in section 3, IBIA uses two parameters, mcs_p and mcs_{im} , which are the maximum clique size constraints for the partition and the approximate CTFs respectively. We expect the error to decrease with an increase in mcs_p , since a larger number of nets are added in each partition. The dependence on mcs_{im} is more complex. If sufficient number of exact marginalizations are possible, the error can be close to zero even for a low value of mcs_{im} . In the worst case, when no exact marginalizations are possible, the error introduced in each approximation step increases as mcs_{im} is lowered. However, it also allows more new nets to be added, reducing the number of partitions. The value of mcs_{im} is thus a trade-off between the error introduced at each approximation step and the number of partitions. Based on results from various benchmarks, we have empirically chosen mcs_{im} to be 5 less than mcs_p .

We compare the results obtained with IBIA using different values of mcs_p and mcs_{im} for all three queries. Table 2 compares the required runtime, the maximum error and the RMSE in MAR_p , MAR_e . Table 3 compares the required runtime and error in $\log(PR)$ (Δ_{IBIA}). We show the results for a subset of benchmarks. The results for others are similar. The number of partitions is indicated in brackets. Owing to memory constraints, we limit our experiments to clique sizes of 25. Similar to all BP based techniques, the clique size bounds should be atleast as large as the CPDs. The size of input CPDs increases with the domain cardinality and in-degree of the variables in the BN. Therefore, some testcases require larger values of mcs_p . These include testcases diabetes and barley where the maximum variable domain cardinality is 21-67 and testcases BN_86, BN_91, BN_93, BN_125 where the maximum in-degree is 16-17. In these cases, mcs_p of 10 and 15 is not possible.

It is seen from Table 2 that, as expected, both the max-error and RMSE reduce or remain almost the same, with increasing mcs_p and mcs_{im} . Except for a few testcases (for example, pedigree18, pedigree30), it is seen that both max-error and RMSE are quite low even when the number of partitions is large. In the benchmark diabetes for example, even with 23 partitions, the maximum error is about 0.05. The RMSE is an order of magnitude lower, indicating that majority of the nodes have very low error. With a single partition, IBIA performs exact inference. In this case, the errors are seen to be of the order of 10^{-14} or less, indicating accuracy of our computations. Even with multiple partitions, the error can be quite low, as for example for error in MAR_p in BN_33 ($\approx 10^{-5}$) and blockmap_05_03-0003 (10^{-15}). This will occur if a larger number of exact marginalizations are possible.

A similar trend in Δ_{IBIA} is observed while estimating PR as shown in Table 3. Here, the errors are very low, except for fs-07. This is a relational BN, in which a lot of determinism is present, which we have not fully exploited. Note that the error in the posterior is due to both the approximation and belief update via back-propagation, whereas the error in PR is only due to the approximation technique. Therefore, we get much better accuracies for the PR than for MAR_e .

The runtime of IBIA depends on the time required for each of the build, infer and approximate operations as well as the number of partitions. Additionally, back propagation of beliefs is needed for MAR_e . The runtime for all steps increases with mcs_p , with inference, approximation and back-belief-update having an exponential dependence. Overall, we expect the runtime to increase with mcs_p . The polynomial time complexity of CT construction is dominant for lower values of mcs_p and the exponential complexity of the other steps dominates for larger values of mcs_p . This is seen for most of the benchmarks in Tables 2 and 3, where there is a significant jump in the runtimes due to larger inference times when mcs_p is increased from 20 to 25. There are occasional fluctuations in this trend. This happens typically when the incremental CT building algorithm struggles to add nets to a partition due to large CPD sizes or the local structure of the network calls for repeated re-triangulation of most of the existing CT. This is seen in BN_60 and a couple of mastermind examples. As expected, the runtime flattens out as the number of partitions approaches one as seen in BN_33 and munin4. While generally comparable, in a few cases the runtime for computation of PR is significantly lower than the run time for posterior marginals (for example in pedigree18 and pedigree30). This is due to the additional time required for belief update via back propagation.

Table 2: Comparison of maximum error, RMSE and required runtime for inference of marginals using various clique size constraints. Number of partitions in each case is indicated in brackets. Entries are marked with ‘-’ when $mcs_p < \text{maximum CPD size}$.

	(mcs _p , mcs _{im})	Maximum Error (#Partitions)				RMSE				Runtime			
		(10,5)	(15,10)	(20,15)	(25,20)	(10,5)	(15,10)	(20,15)	(25,20)	(10,5)	(15,10)	(20,15)	(25,20)
MAR _e	BN_33	0.057 (2)	1×10^{-15} (1)	1×10^{-15} (1)	1×10^{-15} (1)	0.005	1×10^{-16}	1×10^{-16}	1×10^{-16}	1	1	1	1
	BN_42	0.186 (5)	0.131 (5)	0.052 (4)	2E-04 (3)	0.029	0.015	0.008	8e-6	2	4	9	8
	BN_64	0.066 (8)	0.036 (8)	0.009 (8)	0.008 (7)	0.012	0.005	0.001	0.001	9	11	42	752
	BN_49	0.018 (3)	0 (2)	0 (1)	0 (1)	0.002	0	0	0	2	2	1	1
	BN_60	0.403 (7)	0.446 (6)	0.054 (5)	0.008 (5)	0.105	0.122	0.004	7×10^{-4}	7	5	2	25
	BN_66	0.086 (7)	0.069 (8)	0.064 (7)	4×10^{-4} (5)	0.012	0.005	0.005	8×10^{-5}	3	2	7	45
	BN_55	0.049 (4)	0.019 (3)	0.006 (3)	1×10^{-16} (2)	0.006	0.001	9×10^{-4}	8×10^{-18}	3	1	7	6
	BN_86	-	-	6×10^{-9} (2)	1×10^{-13} (1)	-	-	3×10^{-10}	6×10^{-15}	-	-	3	3
	BN_91	-	-	5×10^{-7} (3)	6×10^{-14} (1)	-	-	2×10^{-8}	5×10^{-15}	-	-	3	4
	BN_93	-	-	6×10^{-14} (2)	6×10^{-14} (1)	-	-	8×10^{-15}	8×10^{-15}	-	-	2	3
	pedigree1	0.056 (5)	0.059 (4)	0.005 (2)	1×10^{-14} (1)	0.01	0.00	7×10^{-4}	1×10^{-15}	3	2	1	1
	pedigree23	0.131 (5)	0.128 (5)	0.099 (3)	0.392 (3)	0.017	0.019	0.013	0.025	3	3	3	23
	pedigree18	0.339 (7)	0.186 (7)	0.238 (6)	0.171 (6)	0.046	0.026	0.026	0.021	23	24	31	274
	pedigree30	0.266 (6)	0.213 (8)	0.257 (6)	0.249 (6)	0.046	0.026	0.021	0.027	25	27	39	404
	fs-07	0.016 (4)	0.008 (4)	0.007 (2)	0.006 (2)	0.007	0.005	0.003	0.003	5	3	3	11
	mastermind_04_08_04-0003	0.043 (3)	0.059 (2)	0.008 (2)	3×10^{-16} (1)	0.009	0.008	7×10^{-4}	6×10^{-17}	3	1	2	3
	mastermind_10_08_03-0005	0.013 (5)	0.004 (5)	0.002 (4)	0.001 (3)	0.002	6×10^{-4}	2×10^{-4}	2×10^{-4}	6	2	6	92
	mastermind_10_08_03-0000	0.014 (7)	0.015 (7)	0.011 (7)	0.008 (9)	0.003	0.003	0.002	0.001	26	47	24	467
	mastermind_06_08_03-0000	0.033 (7)	0.028 (5)	0.021 (4)	0.015 (3)	0.006	0.004	0.005	0.003	8	8	32	163
	mastermind_04_08_04-0000	0.049 (7)	0.041 (5)	0.066 (5)	0.051 (5)	0.011	0.008	0.014	0.012	4	41	13	130
	blockmap_10_03-0014	0.505 (12)	0.088 (7)	0.035 (7)	0.033 (5)	0.054	0.004	0.001	0.001	7	6	12	85
MAR _p	Mean	0.101	0.080	0.043	0.043	0.018	0.014	0.005	0.004				
	BN_91	-	-	3×10^{-12} (4)	1×10^{-13} (1)	-	-	2×10^{-13}	8×10^{-15}	-	-	2	11
	BN_93	-	-	3×10^{-11} (2)	8×10^{-14} (1)	-	-	1×10^{-12}	9×10^{-15}	-	-	3	7
	BN_125	-	-	0.001 (10)	2×10^{-14} (1)	-	-	3×10^{-4}	4×10^{-15}	-	-	5	18
	BN_33	0.160 (10)	0.002 (12)	5×10^{-5} (11)	2×10^{-7} (9)	0.009	7×10^{-5}	2×10^{-6}	2×10^{-8}	2	2	4	55
	BN_37	0.061 (11)	0.131 (11)	0.002 (10)	5×10^{-6} (8)	0.005	0.005	2×10^{-4}	1×10^{-7}	2	2	5	66
	BN_40	0.049 (10)	0.009 (11)	0.001 (10)	3×10^{-7} (9)	0.005	5×10^{-4}	4×10^{-5}	2×10^{-8}	2	2	5	71
	BN_43	0.028 (6)	0.017 (5)	0.004 (4)	1×10^{-4} (2)	0.004	0.002	2×10^{-4}	8×10^{-6}	1	1	2	16
	BN_51	0.077 (5)	0.058 (4)	0.035 (3)	1×10^{-16} (2)	0.013	0.007	0.003	9×10^{-18}	2	2	3	49
	BN_55	0.086 (8)	0.086 (9)	0.026 (7)	8×10^{-3} (8)	0.01	0.007	0.002	7×10^{-4}	1	1	3	60
	BN_62	0.094 (7)	0.050 (4)	0.056 (3)	0.038 (3)	0.013	0.007	0.004	0.002	2	2	3	25
	BN_64	0.115 (7)	0.064 (8)	0.011 (8)	0.005 (8)	0.013	0.007	9×10^{-4}	6×10^{-4}	1	1	3	65
	BN_66	0.124 (8)	0.124 (10)	0.113 (10)	0.009 (9)	0.008	0.007	0.007	6×10^{-4}	1	1	4	70
	mastermind_10_08_03-0010	0.042 (10)	0.015 (7)	0.011 (7)	0.008 (9)	0.004	0.003	0.002	0.001	20	46	24	463
	mastermind_06_08_03-0010	0.041 (7)	0.026 (4)	0.021 (4)	0.015 (3)	0.007	0.004	0.005	0.003	8	7	32	162
	mastermind_04_08_03-0010	0.052 (4)	0.030 (3)	0.036 (3)	0.004 (2)	0.013	0.007	0.008	3×10^{-4}	11	10	7	29
	blockmap_05_03-0003	0.603 (9)	0.142 (5)	1×10^{-15} (5)	1×10^{-15} (3)	0.168	0.026	1×10^{-16}	1×10^{-16}	1	1	2	1
	blockmap_15_01-0006	0.602 (20)	0.485 (13)	0.189 (8)	0.113 (9)	0.193	0.111	0.03	0.018	33	41	77	794
	blockmap_10_01-0005	0.364 (15)	0.361 (7)	0.222 (7)	3×10^{-16} (5)	0.12	0.075	0.02	8×10^{-17}	8	12	23	205
	90-42-5	0.021 (11)	0.001 (11)	0.003 (10)	6×10^{-7} (11)	0.002	1×10^{-4}	1×10^{-4}	3×10^{-8}	2	2	5	67
	90-23-5	0.011 (7)	4×10^{-8} (5)	0.002 (4)	5×10^{-8} (4)	0.001	6×10^{-9}	2×10^{-4}	7×10^{-9}	0.5	1	1	11
	andes	7×10^{-4} (4)	9×10^{-6} (3)	1×10^{-5} (2)	3×10^{-15} (1)	8×10^{-5}	9×10^{-7}	1×10^{-6}	3×10^{-16}	0.2	0.3	0.4	2
	barley	-	-	7×10^{-4} (2)	7×10^{-15} (1)	-	-	4×10^{-5}	5×10^{-16}	-	-	0.1	0.2
	munin1	0.142 (4)	0.104 (5)	0.017 (4)	6×10^{-4} (2)	0.009	0.006	0.002	5×10^{-5}	0.2	0.2	0.2	1
	munin3	0.041 (3)	0.005 (2)	5×10^{-4} (2)	2×10^{-15} (1)	0.002	4×10^{-4}	4×10^{-5}	1×10^{-16}	1	1	1	2
	munin4	0.088 (4)	0.055 (3)	2×10^{-4} (2)	2×10^{-15} (1)	0.004	0.002	5×10^{-6}	2×10^{-16}	1	1	1	1
	diabetes	-	0.043 (24)	0.049 (23)	7×10^{-4} (11)	-	0.01	0.005	5×10^{-5}	-	1	1	4
	Mean	0.133	0.082	0.032	0.007	0.029	0.013	0.003	0.001				

Table 3: Comparison of error in PR estimated with IBIA using various clique size constraints. Entries are marked with ‘-’ when $mcs_p < \text{maximum CPD size}$.

	(mcs _p , mcs _{im})	Δ_{IBIA}				Runtime			
		(10,5)	(15,10)	(20,15)	(25,20)	(10,5)	(15,10)	(20,15)	(25,20)
PR	BN_33	-2×10^{-7}	-2×10^{-7}	-2×10^{-7}	-2×10^{-7}	1	1	1	1
	BN_49	7×10^{-7}	7×10^{-7}	7×10^{-7}	7×10^{-7}	1	1	1	1
	BN_60	-0.08	0.1	1×10^{-7}	1×10^{-7}	1	1	2	25
	BN_66	-0.005	0.001	5×10^{-8}	-2×10^{-4}	1	1	3	36
	BN_55	-6×10^{-4}	7×10^{-7}	7×10^{-7}	7×10^{-7}	0.5	1	1	6
	BN_86	-	-	-4×10^{-7}	-4×10^{-7}	-	-	3	3
	BN_91	-	-	-1×10^{-7}	-1×10^{-7}	-	-	2	4
	BN_93	-	-	2×10^{-5}	2×10^{-7}	-	-	2	3
	pedigree1	-4×10^{-3}	-3×10^{-6}	1×10^{-5}	-2×10^{-7}	0.4	0.4	0.4	1
	pedigree23	-0.03	-0.07	9×10^{-5}	1×10^{-5}	1	1	1	4
	pedigree18	-0.3	-0.006	-0.05	-0.002	2	2	2	11
	pedigree30	-0.2	-0.07	-0.01	-0.01	2	2	3	15
	fs-07	1	0.9	0.9	0.6	0.4	0.4	1	3
	mastermind_04_08_04-0003	2×10^{-7}	2×10^{-7}	2×10^{-7}	2×10^{-7}	3	1	2	3
	mastermind_10_08_03-0005	2×10^{-7}	2×10^{-7}	2×10^{-7}	2×10^{-7}	6	2	6	92
	blockmap_10_01-0014	5×10^{-8}	5×10^{-8}	5×10^{-8}	5×10^{-8}	6	7	13	68
	blockmap_10_03-0014	-0.3	0.008	0.007	0.002	4	5	8	49

It is seen from the tables that increasing mcs_p beyond 20 results in a marginal decrease in error with a large increase in runtime. Based on this, we chose $mcs_p = 20$ for further experiments.

8.2 Comparison with other approximate methods

We compared the performance of IBIA with other approximate methods for all three inference queries PR, MAR_e and MAR_p . The details of the datasets, methods and metrics used for evaluation are as follows.

8.2.1 DATASETS

The following datasets were used in this work for evaluation.

1. BN: from UAI06, UAI08, UAI14 (Ihler, 2006), #Instances - 119
We refer to this set as *BN_UAI* in our discussion since we use BN for Bayesian Networks.
2. Relational: from UAI12 dataset (Ihler, 2006), #Instances - 395
Most of these benchmarks have a significant degree of determinism. It includes the following subsets of networks.
 - Mastermind: #Instances - 128
 - Blockmap: #Instances - 240
 - Students: #Instances - 16
 - Friends & Smokers (FS): #Instances - 11
3. Pedigree: from UAI06 (Ihler, 2006), #Instances - 22
These BNs are simplified based on a fixed evidence state; therefore, only posteriors can be computed.
4. Grid-BN: from UAI-06-MPE benchmarks (Dechter, 2006). #Instances - 32
No standard evidence file is available; therefore, only priors can be inferred.
5. Bnlearn: Miscellaneous discrete BNs provided with the bnlearn package for bayesian learning and inference (Scutari, 2007). #Instances - 26
No standard evidence file is available; therefore, only priors can be inferred.

All instances of the above benchmarks are evaluated in this work. The details of benchmarks, including number of nodes, maximum factor size and treewidth are available in Ihler (2006), Scutari (2007).

8.2.2 METHODS USED FOR COMPARISON

Wherever possible, the exact probabilities were estimated using the ACE, which implements the Weighted Model Counting technique (Chavira & Darwiche, 2008). A number of approximate inference algorithms have been implemented in libDAI (Mooij, 2010a) and Merlin tools (Marinescu, 2016). Table 11 in the Appendix has a summary of the results obtained using various algorithms in libDAI, in terms of error, the number of benchmarks solved

and the average runtime for 90 BN_UAI benchmarks. It is seen that Fractional Belief Propagation (FBP) (Wiegerinck & Heskes, 2003) and Tree Re-weighted Belief Propagation (TRWBP) (Wainwright et al., 2003) solve the largest number of cases among the deterministic approximate algorithms, with reasonable errors and runtime. Also, they give an estimate of all the queries of interest. These results agree with the results for PR reported in a recent evaluation of various approximate methods (Agrawal, Pote, & Meel, 2021). As a consistency check, we used both these methods for comparison. We also include a comparison with the method based on Gibbs sampling for some benchmarks.

Merlin includes implementations of Weighted Mini-Bucket elimination (WMB) (Liu & Ihler, 2011) and Iterative Join Graph Propagation (IJGP) (Mateescu et al., 2010). These two methods are based on mini-bucket heuristics. They have a single parameter (*ibound*) that controls the size of the largest permissible cluster, making it suitable for comparison with our method. We used both these methods for comparison.

Both libDAI and Merlin are robust and have been used for comparison with other methods (Agrawal et al., 2021; Lin et al., 2020).

8.2.3 ERROR METRICS AND RUNTIME EVALUATION

The following error metrics were used to evaluate our algorithm.

- Query : Partition Function (PR)
 - *Error in log PR*: $\Delta_{Alg} = \log PR_{Alg} - \log PR_{ACE}$
- Query : Posterior and prior marginals MAR_e , MAR_p
 - *Maximum Error*(max-error): Modulus of the maximum error in probability over all non-evidence variables and states.
 - *Root Mean Square Error* (RMSE): Root mean square error in the probability of all states of all non-evidence variables.
 - *Score* (Mateescu et al., 2010): It is computed as the average KL distance between the exact (P) and approximate (Q) marginal probabilities as follows.

$$Score = 10^{-\frac{1}{N_s} \sum_{s \in N_s} P(s) \log \frac{P(s)}{Q(s)}}$$

where, N_s , is the total number of states over all variables.

This score increases with the accuracy of estimation. It is one when exact marginals are estimated. If a solver is not able to solve the problem, it is assigned a score of zero. To evaluate performance over a benchmark set, we used the method in Mateescu et al. (2010). The sum of the scores (*SumScore*) over all networks in the set is computed as a function of time. It is reflective of both runtimes and the error.

The average KL distance is better than RMSE when the dynamic range of the probabilities is large. On the other hand, the KL distance marks a state as accurate if $P(s) = 0$ and $Q(s) \neq 0$. For states where the $Q(s) = 0$ and $P(s) \neq 0$, the distance becomes infinite. If this happens for even one of the states of the benchmark, the entire benchmark will be

assigned a score of zero. To avoid this, for these states, we set $Q(s) = 10^{-16}$ while computing KL distance. RMSE does not have this problem. For the BN_UAI benchmarks, we have computed both.

Each tool reports the marginals using a different number of precision digits. To compare results of various approximate methods in a consistent manner, we use three decimal places to compute the max-error and RMSE in the marginals.¹ For cases where exact solutions were not available, we have compared our results with the results obtained using the other methods

All experiments were carried out on a 3.7-GHz Intel i7-8700 Linux system with 64-GB memory. More than 500 benchmarks available in Ihler (2006) were used for evaluation of our method. A time limit of one hour was set for each benchmark. While the ACE solver is available as a Java binary executable, source codes written in C++ are available for libDAI and Merlin. IBIA is implemented in Python3 with NetworkX and NumPy libraries.

Table 4 has the details of compile and runtime options used with different inference methods (Chavira & Darwiche, 2015; Mooij, 2010b; Marinescu, 2016). With libDAI, we enabled simplification of the factor graph by setting the *surgery* switch. We have used $mcs_p = 20$ for IBIA. For a fair comparison of the error, we used an *ibound* of 20 for WMB and IJGP. While this is a fair comparison when the networks have only binary variables, this puts WMB and IJGP at an advantage in terms of error for networks that contain variables with domain sizes greater than 2. However, in terms of runtime, this could be a disadvantage for WMB and IJGP since the complexity of message passing is higher. It is partially offset by the fact that our code is implemented in Python, whereas the Merlin tools are compiled C++ codes. Since the cluster sizes in FBP and TRWBP are determined solely by the CPDs, we expect the error to be larger.

In any case, it is not possible to have a fair comparison of the run times. We have included the run times for various methods mainly to show that the run time of IBIA is very competitive.

Table 4: Setup for tools used in our experiments.

Tool	Compiler/ Interpreter	Algorithm	Runtime switches used
IBIA	Python v3.9 (Libraries: NetworkX v2.5, NumPy v1.19.4)	IBIA	$mcs_p=20$, $mcs_{im}=15$
libDAI	g++ v5.4	uai2fg FBP TRWBP	surgery=1 inference=SUMPROD, updates=SEQMAX, logdomain=0, tol=1e-9, maxiter=10000, damping=0.0 updates=SEQFIX, tol=1e-9, maxiter=10000, logdomain=0, nrtrees=0
Merlin	g++ v5.4	WMB, IJGP	ibound=20, iterations=10
ACE	JRE v9-internal	ACE	-Xmx50G (for both compile, evaluate) -e <evidFile> (for compile; while finding posteriors)

1. The format used by various tools for MAR is as follows. ACE - number format with 17 decimal places. libDAI - scientific format with 3 decimal places (X.XXXE-Y). Merlin - number format with 6 decimal places

8.2.4 SIMPLIFICATION OF THE NETWORK

All tools perform some simplification to remove some of the determinism in the network, especially in the presence of evidence. Both determinism and local structure have been exploited very efficiently in ACE (Chavira et al., 2006; Chavira & Darwiche, 2005). libDAI has a switch *surgery*, which reduces the factor graph when set to a non-zero value. However, the exact reduction methods used in these tools are unknown. Similarly, it is not clear what simplification methods is included in Merlin, although Mateescu et al. (2010) indicate that IJGP performs SAT-based variable domain pruning.

For a fair comparison, we also simplified the available input BN using the steps. The first step was to simplify the network based on the fixed state of the evidence and other nodes. For each such node, we removed the outgoing edges and simplified the CPDs of the node and it’s successors. If the reduced CPD of the node contains all ones, it does not affect the product. Moreover, the node is independent of its parents. Therefore, all incoming edges to this node were removed. If the reduced CPD fixes the state of the parent nodes, the same procedure is repeated for the parent nodes. For example, if the reduced CPD of a node with two parents is (0,0,0,1), this implies that the parent nodes are fixed to state 11. This simplification is repeatedly performed until there are no fixed nodes in the BN. Additionally, if a node X is conditionally independent of its parent P given all other parents, the edge between node X and its parent P is removed and the CPD of X is reduced.

We also did structural simplification for nodes with single parents where the CPD enforces either equality (buffer) or negation (inverter) between the node and its parent. All such nodes were collapsed and the successors were connected to the source node. The CPD of the successors is modified to take care of possible inversion. Even though this step results in an increased out-degree for the source node, it can potentially reduce the re-convergence depth (cycle length), leading to a lower tree-width.

In all our experiments, we used the available network files directly as input to all tools. The runtimes indicated include the time required for simplification.

8.2.5 SUMMARY OF RESULTS

For the BN_UAI benchmarks, we have tabulated detailed results, including max-error and RMSE in MAR_e , MAR_p , and error in $\log(PR)$. We have also tabulated runtimes and included plots for the *SumScore*. For other benchmarks, we have plotted histograms of the maximum error and the *SumScore* as a function of time. The *SumScore* plots give a concise description of error and runtimes.

The following summarizes the observations from our evaluations:

- Table 5 contains the number of instances of each benchmark that can be solved by each method. IBIA gives solutions for PR and MAR_e for 523/536 benchmarks, which is better than ACE, WMB, TRWBP, and IJGP. For MAR_p , IBIA solves 565/572 benchmarks, which is better than ACE, WMB and IJGP and marginally lower than FBP and TRWBP, which give solutions for all 572.
- For BN_UAI benchmarks, we have tabulated detailed data for error in $\log(PR)$ (Table 6), max-error and RMSE in MAR_e (Table 8) and MAR_p (Table 10). We have done this for two different values of mcs_p and mcs_{im} . In all cases, IBIA results in

significantly lower errors. On an average, both max-error and RMSE is an order of magnitude lower and the error in PR is several orders of magnitude lower than other approximate methods.

- For Relational, Pedigree, Grid-BN and Bnlearn benchmarks, we have plotted histograms of error in $\log(PR)$ and maximum error in MAR_e and MAR_p in Figures 7, 8 and 11 respectively. We have also plotted the *SumScore* as a function of runtime constraint in Figures 9 and 12. The max-error is once again significantly lower than other methods. The *SumScore* is comparable or better.
- For BN_UAI testcases where exact solutions are not available, we have compared the solutions obtained by the approximate methods. Table 7 has the *PR* and Figures 10 and 13 has the results for MAR_e and MAR_p . We find that the difference in the marginals obtained by various approximate methods is lower for the priors than the posteriors.
- Tables 9, 10 have runtimes for BN_UAI benchmarks. Our method is very competitive despite it being implemented in Python.

Table 5: List of benchmarks and the corresponding total number of instances evaluated for different probabilistic queries. For each set, we compare the number of instances that successfully run with different inference algorithms.

Query	Benchmark	Total	ACE	FBP	TRWBP	WMB	IJGP	IBIA
PR, MAR_e	BN_UAI	119	90	119	116	106	101	117*
	Pedigree	22	9	22	22	7	12	22*
	Relational	395	395	392	348	227	203	384
	Total	536	494	533	486	340	316	523
MAR_p	BN_UAI	119	76	119	119	105	94	119*
	Grid-BN	32	29	32	32	32	26	32
	Relational	395	386	395	395	196	170	388
	Bnlearn	26	26	26	26	26	26	26
	Total	572	517	572	572	359	316	565

* Three BN_UAI and two Pedigree inferred with $mcsim = 10$.

We now present detailed comparisons of results obtained with different methods for each probability query.

8.2.6 PR: PROBABILITY OF EVIDENCE, $P(e)$

To evaluate the accuracy of the estimated PR, we first considered the subset of BN_UAI benchmarks where exact probabilities could be found using ACE. Table 6 contains the PR obtained using ACE and the error in estimates ($\Delta_{Alg} = \log PR_{Alg} - \log PR_{ACE}$) obtained by the approximate algorithms. Benchmarks for which all methods give accurate results are not included here.

Table 6: Exact probability of evidence obtained using the ACE solver (PR_{ACE}) and the error in PR estimated using different approximate inference techniques ($\Delta_{Alg} = \log PR_{Alg} - \log PR_{ACE}$) for various BN_UAI benchmarks. Entries are marked with ‘-’ for testcases where inferred PR is > 1 .

Benchmark	$\log PR_{ACE}$	Δ_{FBP}	Δ_{TRWBP}	Δ_{WMB}	Δ_{IBIA}
BN_105	-0.83	0.12	0.12	8×10^{-8}	-9×10^{-7}
BN_107	-1.15	-0.07	-0.07	0.22	-2×10^{-7}
BN_109	-1.89	-0.20	-0.20	1×10^{-7}	3×10^{-7}
BN_111	-1.28	0.14	0.14	7×10^{-8}	-2×10^{-7}
BN_113	-1.75	-0.11	-0.11	2×10^{-7}	0
BN_2	-7.52	-0.02	-0.02	0.10	4×10^{-7}
BN_22	-304.14	0.66	0.66	6×10^{-8}	0
BN_23	-304.14	0.66	0.66	6×10^{-8}	0
BN_24	-297.7	4.07	4.07	2×10^{-7}	-7×10^{-7}
BN_25	-297.7	4.07	4.07	2×10^{-7}	-7×10^{-7}
BN_30	-10.99	-0.21	-0.21	3.05	-4×10^{-7}
BN_31	-10.99	-0.21	-0.21	4.59	-4×10^{-7}
BN_32	-11.55	-0.20	-0.20	4.42	-2×10^{-7}
BN_33	-11.55	-0.20	-0.20	4.88	-2×10^{-7}
BN_34	-14.39	0.55	-0.01	3.26	1×10^{-7}
BN_35	-14.39	0.51	-0.35	3.92	1×10^{-7}
BN_36	-9.26	-1.11	-	2.83	2×10^{-7}
BN_37	-9.26	-1.11	-1.13	3.51	2×10^{-7}
BN_38	-10.29	-1.41	-1.40	3.95	0
BN_39	-10.29	-1.42	-0.97	4.49	0
BN_40	-13.21	-1.73	-1.41	2.82	7×10^{-8}
BN_41	-13.21	-1.73	-1.55	1.83	7×10^{-8}
BN_42	-2.37	-0.16	-0.16	0.20	-5×10^{-7}
BN_43	-2.31	-0.51	-	0.47	-4×10^{-5}
BN_44	-3.69	-0.05	-0.05	0.18	-8×10^{-7}
BN_45	-1.89	-0.56	-0.76	0.07	1×10^{-6}
BN_46	-2.72	3×10^{-5}	3×10^{-5}	0.40	7×10^{-7}
BN_47	-2.08	-0.15	-0.15	-	-5×10^{-8}
BN_48	-2.08	-0.15	-0.15	-	-5×10^{-8}
BN_49	-1.72	-0.09	-0.09	-	7×10^{-7}
BN_50	-1.72	-0.09	-0.09	-	7×10^{-7}
BN_51	-1.43	-0.08	-0.08	-	2×10^{-7}
BN_52	-1.43	-0.08	-0.08	-	2×10^{-7}
BN_53	-1.13	0.007	0.007	-	2×10^{-7}
BN_54	-1.13	0.007	0.007	-	7×10^{-6}
BN_55	-1.74	0.02	0.02	-	7×10^{-7}
BN_56	-1.74	0.02	0.02	-	7×10^{-7}
BN_57	-1.93	0.005	0.005	-	2×10^{-6}
BN_58	-1.93	0.005	0.005	-	2×10^{-6}
BN_59	-2.47	-0.28	-0.28	-	1×10^{-7}
BN_60	-2.47	-0.28	-	-	1×10^{-7}
BN_61	-1.71	0.03	0.03	-	1×10^{-6}
BN_62	-1.71	0.03	0.03	-	1×10^{-6}
BN_63	-0.73	0.02	0.02	-	-4×10^{-5}
BN_64	-0.73	0.02	0.02	-	-1×10^{-5}
BN_65	-1.07	-0.30	-0.30	-	5×10^{-8}
BN_66	-1.07	-0.30	-0.30	-	5×10^{-8}
BN_67	-0.49	-0.01	-0.01	-	-5×10^{-5}
BN_68	-0.49	-0.01	-0.01	-	-1×10^{-5}
BN_8	-2.39	0.003	0.003	0.15	4×10^{-6}
Mean $ \Delta_{Alg} $		0.48	0.44	1.62	4×10^{-6}

It is seen from the table that IBIA has a mean error of the order of 10^{-6} and maximum of 10^{-5} , both of which are several orders of magnitude lower than the other methods. Further, although the mean errors obtained with FBP, TRWBP are of the order of 10^{-1} , the errors for some testcases like BN_24, BN_25 are as large as 4. IJGP does not give PR, while WMB gives upper bounds for PR. Therefore, the errors obtained with WMB are always positive. Although the bound is good in many cases, it is worse than the LBP variants for BN_30-40. There are also many cases for which the estimates obtained by WMB are greater than one, which are marked with a dash in the table.

Figure 7 has histograms of the maximum error in $\log(PR)$ obtained using various methods for the Relational and Pedigree benchmarks. ACE finds a solution for 404 benchmarks, which includes all the relational benchmarks which have a lot of determinism and 9 Pedigree benchmarks. The errors are within ± 0.5 in 379 out of 393 benchmarks solved by IBIA, as opposed to 302 out of 401, 286 out of 357, and 147 out of 232 benchmarks solved by FBP, TRWBP and WMB respectively. The error is outside the range of plots for 4 cases with FBP and 33 cases with WMB. The maximum error over all benchmarks is about 4 with IBIA, while it is 42 with WMB, 9 with TRWBP and 15 with FBP.

The exact PR for some of the Pedigree benchmarks are reported in Gogate and Dechter (2011). For these cases, the estimates obtained with IBIA are within two decimal places of the exact results.

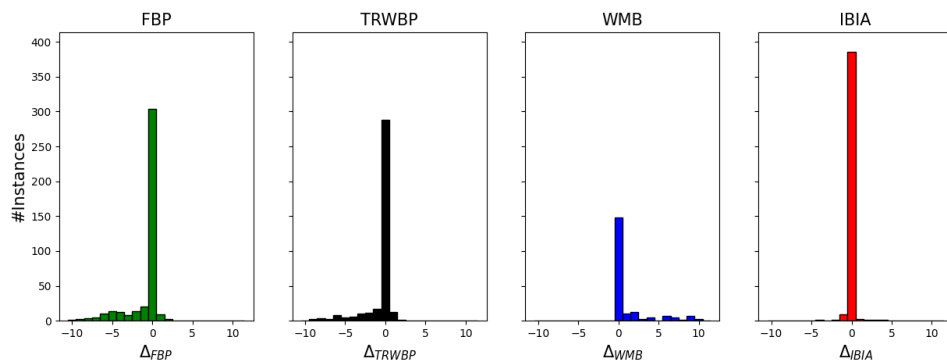


Figure 7: Histogram of errors in PR ($\Delta_{Alg} = \log PR_{Alg} - \log PR_{ACE}$) obtained using various approximate inference techniques for Relational and Pedigree benchmarks. Errors outside the range $(-10.5, 10.5)$ are not plotted. Bin-size=1
Instances - #ACE:404, #FBP:401, #TRWBP:357 #WMB:232 #IBIA:393

ACE does not give solutions for 29 of the BN_UAI benchmarks. For these cases, we compared the PR obtained using IBIA with the values obtained using other approximate methods. Table 7 has the results of the comparison. In majority of the cases, the PR estimated using IBIA match those obtained with FBP and TRWBP to within two decimal places. Also, it is seen that TRWBP and FBP agree reasonably well except for BN_70, where there is a difference of 15. There are significant differences with WMB for a few benchmarks like BN_129 and BN_132, but this is expected since it computes the upper bound. Estimates of PR obtained using IBIA are higher than those obtained using FBP

and TRWBP in testcases BN_69-BN_77. For these benchmarks, the last column contains exact values reported in Gogate and Dechter (2011). It is seen that IBIA gives better estimates than FBP and TRWBP in all these cases. From the results reported in Gogate and Dechter (2011), it also gives better estimates than the edge-deletion-belief-propagation (EDBP) algorithm proposed in Choi and Darwiche (2006). However, our estimates are worse than the IJGP with sample search proposed in Gogate and Dechter (2011) for some cases. WMB fails to give estimates for these benchmarks.

Table 7: Comparison of $\log(PR)$ obtained using different approximate inference methods for BN_UAI testcases for which ACE does not work. The maximum difference in estimates obtained with IBIA and other methods is also indicated. Entries are marked with ‘-’ for testcases where inferred PR > 1 and with ‘UF’ where an underflow error occurs.

Benchmark	FBP	TRWBP	WMB	IBIA	Exact ¹
BN_12	-3.61	-3.61	-3.31	-3.61	
BN_126	-55.68	-55.68	-54.26	-55.78	
BN_127	-57.5	-57.5	-55.94	-57.68	
BN_128	-47.29	-47.29	-47.27	-47.32	
BN_129	-61.06	-61.06	-56.57	-61.9	
BN_13	-2.32	-2.32	-1.98	-2.32	
BN_130	-57.41	-57.41	-56.59	-57.46	
BN_131	-53.98	-53.98	-53.27	-53.69	
BN_132	-64.1	-64.1	-58.61	-64.44	
BN_133	-53.64	-53.64	-51.82	-53.32	
BN_134	-56.2	-56.2	-54.62	-56.86	
BN_15	-5.7	-5.7	-5.33	-5.7	
BN_16	-0.08	-0.08	-0.01	-0.08	
BN_17	-0.08	-0.08	-0.05	-0.08	
BN_18	-0.09	-0.09	-	-0.09	
BN_19	-0.09	-0.09	0	-0.09	
BN_20	-410.5	-410.5	-	UF	
BN_21	-410.5	-410.5	-	UF	
BN_26	-974.12	-974.12	-	-973.99	
BN_27	-974.12	-974.12	-	-973.99	
BN_69	-60.45	-60.19	-	-54.79	-53.28
BN_70	-77.56	-93.42	-	-75.14	-70.7
BN_71	-118.26	-117.61	-	-111.94*	-110.29
BN_72	-155.69	-156.39	-	-153.07	-149.38
BN_73	-118.21	-119.34	-	-114.11	-112.65
BN_74	-48.73	-48.73	-	-47.04*	-44.43
BN_75	-98.02	-97.8	-	-92.37	-90.23
BN_76	-115.04	-115.7	-	-111.06	-109.31
BN_77	-83.65	-86.77	-	-81.12*	

¹ Exact values for some benchmarks are reported in Gogate and Dechter (2011)

*Testcases inferred using $mcs_{im} = 10$

8.2.7 MAR_e : POSTERIOR MARGINALS, $P(X|e)$

The next inference task we consider is the computation of posterior node marginals.

Table 8 compares the maximum error and RMSE obtained with different inference algorithms for a subset of BN_UAI testcases for which exact solutions are available. Small networks where all methods give accurate results are not tabulated here. In order to see the

effect of clique sizes used in IBIA, we present results obtained with two sets of clique size constraints: $mcs_p = 20$, $mcs_{im} = 15$ and $mcs_p = 15$, $mcs_{im} = 10$.

It is seen from the table that IBIA results in the least average max-error and RMSE compared to other methods for both sets of clique size constraints. With $mcs_p = 20$, the average max-error over all benchmarks is 0.008 and the average RMSE is 0.001, an order of magnitude lower than that achieved with other methods. The maximum error obtained with IBIA is 0.06, with zero error in a large number of cases. As discussed, an error of zero, means that the marginals are accurate to 3 decimal places.

When mcs_p is reduced to 15, both max-error and RMSE increase, but continue to be lower than other methods for most cases. The maximum error is around 0.1 or lower in all cases except BN_59, BN_60, where it increases to 0.45 and 0.62 which is comparable to the error obtained using the other methods. Testcases BN_90 and BN_91 could not be inferred with $mcs_p = 15$, since the maximum CPD size is 17 ($> mcs_p$).

IBIA is expected to give lower errors than FBP and TRWBP, due to larger cluster sizes. However, it also gives significantly lower errors than WMB and IJGP which are run with comparable or larger cluster sizes. We also note that although max-errors are greater than 0.5 for quite a few cases with FBP, TRWBP, WMB and IJGP, the mean RMSE is less than 0.15. This indicates that a large percentage of nodes have small errors with all approximate techniques.

Table 9 compares the runtime required for inference of posteriors using different methods. Though runtimes for different methods are not directly comparable since they are implemented in different programming languages, it gives a decent overall idea. We note that even though IBIA is implemented in Python, the runtimes are quite competitive when compared to other tools. It is better than WMB and IJGP for all benchmarks. This is probably due to the setting of the *ibound* parameter, which was set to get a fair comparison of the error. It is faster than FBP for benchmarks with maximum in-degree between 5-19 (e.g., BN_105, BN_107, BN_86, BN_87, BN_90, BN_91). Our runtimes are also an order of magnitude lower than ACE for some benchmarks like BN_14, BN_2, BN_8, BN_86, etc.

It is also interesting that TRWBP has a lower runtime than FBP for many cases.

Figure 8 has the histograms of maximum error in posterior marginals obtained using different methods for the Pedigree and Relational benchmarks. We have also included the results obtained using Gibbs sampling with 10^4 samples, although the error is much larger than the deterministic approximate methods. For the Pedigree benchmarks, IBIA and WMB have a lower maximum error (< 0.5) than FBP, TRWBP and IJGP. Although the maximum error obtained using IBIA for Pedigree is more distributed than for other benchmarks, it's performance is comparable to WMB, even though it is at a disadvantage with respect to number of variables in a cluster. IBIA also performs significantly better for relational benchmarks. The maximum error is < 0.05 in 65% of the benchmarks with IBIA, whereas with other methods the error is in this range in less than 35% of the benchmarks. Although FBP solves more number of testcases, the errors obtained are larger.

Figure 9 plots the variation of *SumScore* obtained using various approximate inference methods as the timeout constraint is varied for different benchmark sets. Across benchmarks, IBIA has a comparable or better *SumScore* than other methods. For Pedigree, we get a score that is close to 9, which is the perfect score. Though the max-error obtained with both IBIA and WMB is ≈ 0.5 (Figure 8), the average RMSE for these methods is < 0.03 .

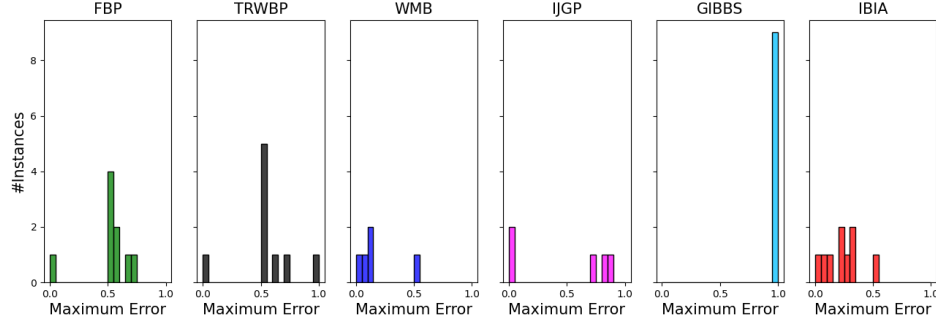
Table 8: Comparison of absolute value of the maximum error and RMSE in MAR_e for BN_UAI benchmarks. For IBIA, errors are reported for two sets of clique size constraints: $mcs_p = 20$, $mcs_{im} = 15$ and $mcs_p = 15$, $mcs_{im} = 10$. Entries are marked with ‘-’ where inference fails. For consistency in precision across algorithms, the error is reported as zero if accurate to three decimal places.

Benchmark	Maximum Error						RMSE					
	FBP	TRWBP	WMB	IJGP	IBIA		FBP	TRWBP	WMB	IJGP	IBIA	
					$mcs_p = 20$	$mcs_p = 15$					$mcs_p = 20$	$mcs_p = 15$
BN_105	0.411	0.411	0	0	0	0	0.15	0.15	0	0	0	0
BN_107	0.149	0.149	0.337	0.194	0	0	0.042	0.042	0.077	0.056	0	0
BN_109	0.272	0.272	0	0	0	0	0.111	0.111	0	0	0	0
BN_111	0.344	0.344	0	0	0	0	0.117	0.117	0	0	0	0
BN_113	0.212	0.212	0	0.489	0	0	0.088	0.088	0	0.184	0	0
BN_14	0.019	0.019	0.01	0.641	0.012	0.017	0.003	0.003	0.002	0.142	0.002	0.003
BN_2	0.015	0.015	0.033	0.53	0.001	0.005	0.003	0.003	0.009	0.222	0	0
BN_22	0.397	0.397	0	0	0	0.029	0.017	0.017	0	0	0	0.002
BN_23	0.397	0.397	0	0	0	0.029	0.017	0.017	0	0	0	0.002
BN_24	0.127	0.127	0	0	0	0	0.016	0.016	0	0	0	0
BN_25	0.127	0.127	0	0	0	0	0.016	0.016	0	0	0	0
BN_30	0.515	0.515	0.362	0.59	0	0	0.077	0.077	0.057	0.107	0	0
BN_31	0.515	0.515	0.447	0.735	0	0	0.077	0.077	0.058	0.126	0	0
BN_32	0.622	0.622	0.433	0.509	0	0	0.114	0.114	0.069	0.097	0	0
BN_33	0.622	0.622	0.668	0.925	0	0	0.114	0.114	0.077	0.133	0	0
BN_34	0.952	0.991	0.493	0.746	0	0	0.146	0.139	0.062	0.123	0	0
BN_35	0.952	0.933	0.694	0.869	0	0	0.141	0.107	0.077	0.123	0	0
BN_36	0.719	-	0.567	0.642	0	0	0.103	-	0.051	0.107	0	0
BN_37	0.719	1	0.663	0.597	0	0	0.103	0.122	0.071	0.109	0	0
BN_38	1	1	0.567	0.798	0	0	0.119	0.136	0.071	0.166	0	0
BN_39	1	0.605	0.375	0.689	0	0	0.119	0.096	0.054	0.133	0	0
BN_40	0.817	0.668	0.395	0.629	0	0	0.114	0.107	0.051	0.080	0	0
BN_41	0.817	0.668	0.314	0.536	0	0	0.114	0.12	0.044	0.085	0	0
BN_42	0.261	0.5	0.049	0.831	0.052	0.131	0.043	0.061	0.011	0.214	0.008	0.015
BN_43	0.286	-	0.187	0.658	0.003	0.047	0.067	-	0.039	0.157	0	0.006
BN_44	0.193	0.193	0.08	0.596	0	0.027	0.039	0.039	0.022	0.210	0	0.004
BN_45	0.332	0.5	0.059	0.469	0	0.007	0.041	0.077	0.013	0.111	0	0.001
BN_46	0.026	0.026	0.3	0.5	0	0	0.003	0.003	0.044	0.164	0	0
BN_47	0.307	0.307	0.53	0.765	0	0.050	0.1	0.1	0.135	0.203	0	0.003
BN_48	0.307	0.307	0.767	-	0	0.050	0.1	0.1	0.168	-	0	0.005
BN_49	0.179	0.179	0.409	0.59	0	0	0.051	0.051	0.098	0.162	0	0
BN_50	0.179	0.179	0.378	0.59	0	0	0.051	0.051	0.083	0.163	0	0
BN_51	0.204	0.204	0.587	-	0	0	0.066	0.066	0.186	-	0	0
BN_52	0.204	0.204	0.636	-	0	0	0.066	0.066	0.213	-	0	0
BN_53	0.183	0.183	0.421	-	0.020	0.072	0.044	0.044	0.138	-	0.001	0.009
BN_54	0.183	0.183	0.387	0.871	0.015	0.044	0.044	0.044	0.132	0.300	0.001	0.004
BN_55	0.191	0.191	0.525	0.875	0.006	0.019	0.038	0.038	0.14	0.244	0.001	0.001
BN_56	0.191	0.191	0.426	0.858	0.006	0.019	0.038	0.038	0.137	0.243	0.001	0.001
BN_57	0.179	0.179	0.362	-	0.005	0.021	0.026	0.026	0.091	-	0	0.002
BN_58	0.179	0.179	0.311	0.806	0	0.021	0.026	0.026	0.094	0.301	0	0.002
BN_59	0.5	0.5	0.613	-	0.054	0.622	0.164	0.164	0.153	-	0.004	0.125
BN_60	0.5	-	0.513	-	0.054	0.446	0.164	-	0.15	-	0.004	0.122
BN_61	0.105	0.105	0.148	-	0	0	0.016	0.016	0.028	-	0	0
BN_62	0.105	0.105	0.151	-	0	0	0.016	0.016	0.033	-	0	0
BN_63	0.184	0.184	0.574	0.884	0.007	0.051	0.033	0.033	0.161	0.260	0.001	0.006
BN_64	0.184	0.184	0.58	0.924	0.009	0.036	0.033	0.033	0.16	0.312	0.001	0.005
BN_65	0.496	0.496	0.649	0.749	0.033	0.062	0.071	0.071	0.202	0.195	0.003	0.006
BN_66	0.496	0.496	0.726	0.96	0.064	0.069	0.071	0.071	0.212	0.233	0.005	0.005
BN_67	0.086	0.086	0.717	0.876	0.040	0.018	0.013	0.013	0.22	0.222	0.005	0.003
BN_68	0.086	0.086	0.638	0.83	0.021	0.018	0.013	0.013	0.207	0.191	0.002	0.003
BN_8	0.031	0.031	0.054	0.556	0.002	0.028	0.004	0.004	0.009	0.251	0	0.003
BN_86	0	0	0	0.273	0	-	0	0	0	0.014	0	-
BN_87	0	0	0	0.5	0	-	0	0	0	0.030	0	-
BN_9	0.025	0.025	0.055	0.624	0.019	0.016	0.003	0.003	0.007	0.207	0.002	0.002
BN_90	0	0	0	0.357	0	-	0	0	0	0.019	0	-
BN_91	0	0	0	0.357	0	-	0	0	0	0.019	0	-
BN_95	0.119	0.119	0	0	0.006	0.018	0.032	0.032	0	0	0.001	0.003
Mean	0.320	0.310	0.319	0.550	0.008	0.037	0.060	0.057	0.072	0.134	0.001	0.006

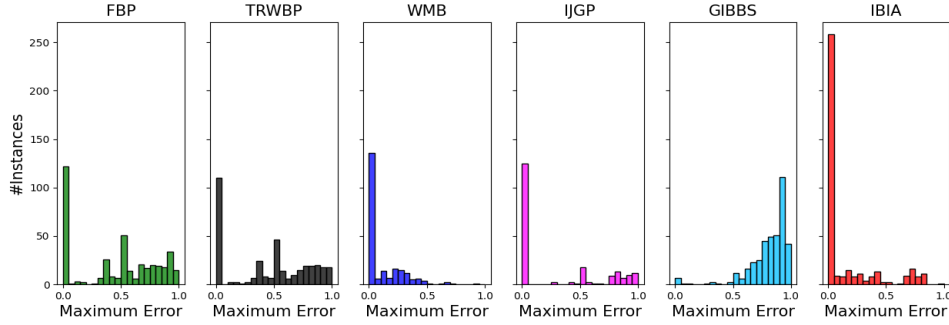
Table 9: Comparison of runtime required (in seconds) to estimate posterior node marginals using different inference algorithms for BN_UAI. For IBIA, runtimes are reported for two sets of clique size constraints: $mcs_p = 20$, $mcs_{im} = 15$ and $mcs_p = 15$, $mcs_{im} = 10$. Entries are marked with ‘-’ where inference fails.

Benchmark	ACE			FBP	TRWBP	WMB	IJGP	IBIA	
	Compile*	Evaluate	Total					$mcs_p = 20$	$mcs_p = 15$
BN_105	3	1	4	22	2	50	49	11	11
BN_107	3	1	4	365	7	168	139	9	9
BN_109	2	1	3	301	5	39	38	8	8
BN_111	2	1	3	209	7	34	34	8	7
BN_113	2	1	3	715	8	150	119	8	8
BN_14	8	24	32	0.01	0.00	63	26	3	1
BN_2	6	20	26	0.01	0.01	69	41	0.3	0.4
BN_22	3	1	4	5	11	19	11	5	47
BN_23	5	2	7	7	13	18	11	5	40
BN_24	2	1	3	8	3	9	7	4	4
BN_25	4	2	6	8	3	43	9	4	4
BN_30	0.4	0.1	0.5	0.1	1	576	341	1	1
BN_31	0.4	0.1	0.5	0.1	1	438	390	1	1
BN_32	1	0.1	1.1	0.2	5	606	510	1	1
BN_33	0.5	0.1	0.6	0.2	2	579	474	1	1
BN_34	0.5	0.1	0.6	84	32	707	478	1	1
BN_35	0.5	0.1	0.6	88	32	492	442	1	1
BN_36	0.4	0.1	0.5	89	-	670	455	1	1
BN_37	0.4	0.1	0.5	91	2	549	500	1	1
BN_38	0.5	0.1	0.6	85	32	594	414	1	1
BN_39	0.5	0.1	0.6	84	32	491	435	1	1
BN_40	0.4	0.1	0.5	0.1	1	626	439	1	1
BN_41	0.4	0.1	0.5	0.1	0.4	510	475	1	1
BN_42	2	4	6	26	16	68	64	9	3
BN_43	1	1	2	36	-	129	89	2	1
BN_44	2	1	3	0.1	0.2	89	71	0.4	2
BN_45	2	3	5	30	16	89	82	1	1
BN_46	1	1	2	0.01	0.01	114	89	0.3	0.3
BN_47	0.3	0.1	0.4	1	1	660	525	2	9
BN_48	0.3	0.1	0.4	1	1	647	-	2	9
BN_49	0.3	0.1	0.4	0.3	0.4	778	564	1	2
BN_50	0.3	0.1	0.4	0.3	0.4	734	510	1	1
BN_51	0.3	0.1	0.4	0.4	0.5	701	-	1	1
BN_52	0.3	0.1	0.4	0.4	0.5	590	-	1	1
BN_53	0.4	0.1	0.5	0.05	0.1	477	-	15	6
BN_54	0.4	0.1	0.5	0.05	0.1	415	293	19	5
BN_55	0.3	0.1	0.4	0.05	0.1	525	348	6	1
BN_56	0.3	0.1	0.4	0.04	0.1	447	319	8	1
BN_57	0.3	0.1	0.4	0.02	0.04	561	-	1	0.4
BN_58	0.3	0.1	0.4	0.02	0.04	457	335	1	0.4
BN_59	0.3	0.1	0.4	0.3	0.2	561	-	2	5
BN_60	0.3	0.1	0.4	0.3	-	551	-	2	5
BN_61	0.3	0.1	0.4	0.2	0.1	765	-	1	1
BN_62	0.3	0.1	0.4	0.1	0.1	680	-	1	1
BN_63	0.5	0.1	0.6	0.1	0.1	519	477	40	12
BN_64	1	0.1	1.1	0.1	0.1	578	325	42	11
BN_65	1	0.1	1.1	0.03	0.04	474	345	4	2
BN_66	0.4	0.1	0.5	0.03	0.03	423	322	7	3
BN_67	0.5	0.1	0.6	0.03	0.03	438	305	14	3
BN_68	0.5	0.1	0.6	0.03	0.03	382	209	7	3
BN_8	42	131	173	0.01	0.005	101	92	3	1
BN_86	6	14	20	19	1	213	162	3	-
BN_87	4	13	17	28	1	242	156	3	-
BN_9	36	113	149	0.01	0.005	67	60	2	1
BN_90	6	15	21	103	1	109	95	2	-
BN_91	6	14	20	26	1	114	81	3	-
BN_95	1	4	5	0.01	0.004	5	5	0.2	0.2

*Compilation performed with evidence



(a) Pedigree (Instances - #ACE/FBP/TRWBP/Gibbs/IBIA:9, #WMB/IJGP:5)



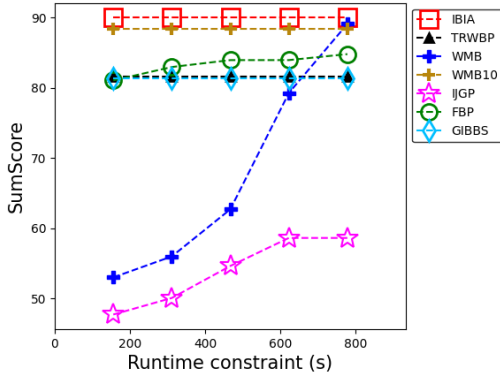
(b) Relational (Instances - #ACE/Gibbs:395, #FBP:392, #TRWBP:348, #WMB:227, #IJGP:203, #IBIA:384)

Figure 8: Histogram of maximum error in posterior node marginals estimated with various approximate inference techniques. The total number of instances that run with ACE and other approximate inference techniques are indicated for each benchmark set. Bin-size=0.05

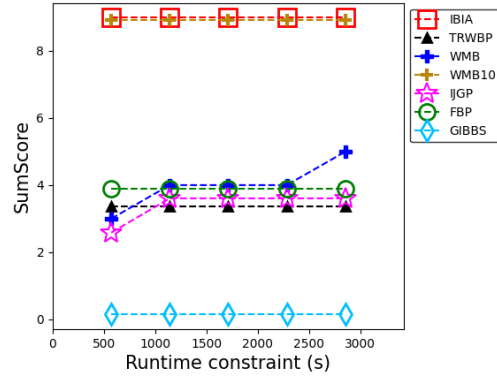
So, the scores achieved are very close to the number of testcases solved by these methods. Also for Pedigree and BN_UAI benchmarks, WMB gets a higher final score than FBP and TRWBP, even though it solves fewer benchmarks indicating it has a lower average error. This is consistent with the histograms in Figure 8. Gibbs sampling performs very poorly with Pedigree benchmarks.

Since WMB with *ibound* = 20 timed out for the remaining Pedigree cases, we ran it with an *ibound* of 10. It is denoted as WMB10 in the figure. WMB with *ibound* = 10 solves more testcases than with *ibound* = 20 within the time limit and achieves close to perfect scores for BN_UAI and Pedigree benchmarks. This is interesting since for BN_UAI both the max-error and RMSE obtained with WMB (*ibound* = 20) are an order of magnitude higher than IBIA (see Table 8). Generally, we have found that if the RMSE is less than 0.1, the score is close to the perfect score. As expected, we found that the max-error for WMB increased when *ibound* was lowered to 10.

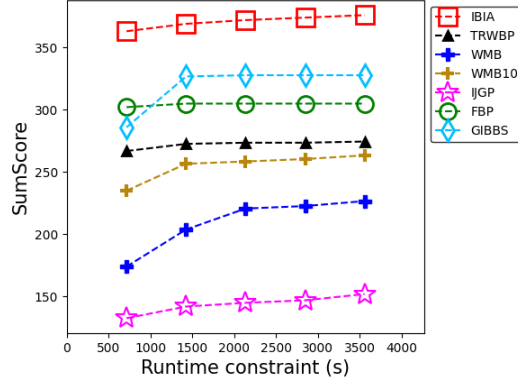
For the relational benchmarks, IBIA has the highest score, once again close to the number of benchmarks solved. WMB also gets a score close to the number of benchmarks solved by it, indicating low error on an average. Gibbs sampling gets a much better score for relational



(a) BN_UAI
(Instances - #ACE/FBP/Gibbs/IBIA:90,
#TRWBP:87, #WMB/WMB10:90 #IJGP:81)



(b) Pedigree
(Instances - #ACE/FBP/TRWBP/WMB10/Gibbs/IBIA:9,
#WMB/IJGP:5)



(c) Relational
(Instances - #ACE/Gibbs:395, #FBP:392, #TRWBP:348,
#WMB:227, #WMB10:272, #IJGP:203, #IBIA:384)

Figure 9: Variation of *SumScore* for posterior marginals obtained using various approximate inference techniques with different timeout constraints. The total number of instances that run with ACE and other approximate inference techniques are indicated for each benchmark set.

benchmarks. However, the score is much lower than number of cases solved by it. For all benchmarks, even though FBP and TRWBP run successfully for a comparable number of instances as IBIA, the scores obtained are smaller, indicating a larger error in estimation. IJGP has a significantly lower *SumScore* as compared to other methods for BN_UAI and Relational benchmarks, partly due to the smaller number of cases for which a solution is obtained.²

2. IJGP returns inconsistent evidence or underflow errors for many testcases.

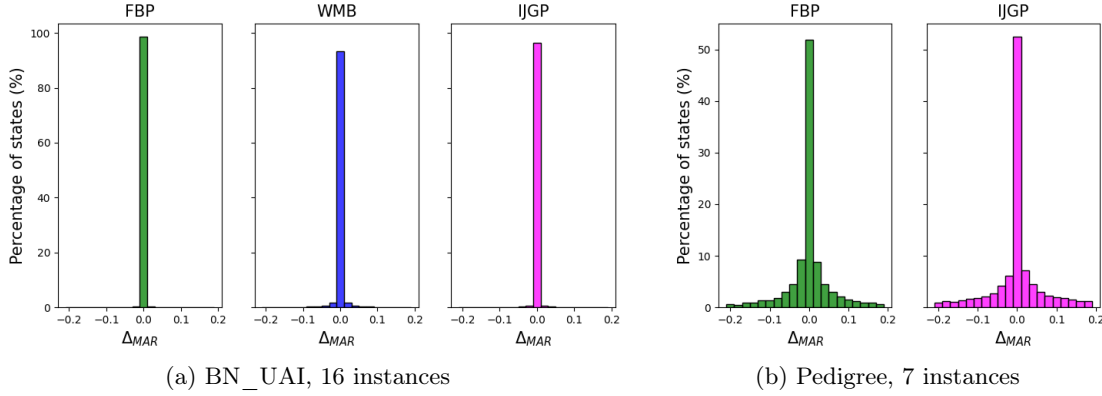


Figure 10: Distribution of difference in posterior node marginals ($\Delta_{MAR} = MAR_{IBIA} - MAR_{Alg}$) for testcases where exact marginals cannot be computed using ACE. Bin-size=0.02

To evaluate cases where ACE does not run, we found the difference in the marginals obtained using IBIA and FBP, IBIA and WMB, IBIA and IJGP. Figure 10 shows the distribution of this difference for 16 instances of BN_UAI and 7 instances of Pedigree where solutions could be obtained using all compared techniques. We observe that for more than 85% of the states of BN_UAI, the marginal distribution obtained with IBIA is within ± 0.01 of that obtained with FBP, WMB and IJGP. The maximum difference in marginals is 0.81 for FBP, 0.98 for WMB and 1.0 for IJGP. For the Pedigree benchmarks, the difference in marginals is within ± 0.01 for slightly more than 50% states. Since WMB solves only two instances, we ignore it while plotting. For Pedigree, the maximum difference in marginals is 0.79 for FBP and 0.96 for IJGP.

8.2.8 MAR_p : PRIOR MARGINALS, $P(X)$

We now discuss the results obtained for prior marginals. We have also reported some additional results for circuit benchmarks in a preliminary version of this paper in Bathla and Vasudevan (2021). We now discuss the results for benchmarks listed in section 8.2.1. As shown in Table 5, ACE solves fewer prior testcases when compared to posteriors. This is because network sizes are larger, with fewer simplifications possible.

Table 10 has the maximum error, the RMSE, and the runtime required to obtain prior marginals using different inference techniques for BN_UAI testcases. We ignore cases where accurate results are obtained with all cases. Once again, both the average max-error and RMSE obtained with IBIA are an order of magnitude lower than with other methods. Even though the number of partitions is increased when compared to posteriors due to reduced simplifications, the max-error is larger than 0.05 only in six cases, and even here it is about 0.1. Errors are obtained with FBP and TRWBP are identical.

In many cases, the runtime required for IBIA is orders of magnitude smaller than ACE, WMB, and IJGP. Once again, this is also partially due to the setting of the *ibound* parameter in WMB and IJGP. It is also lower than FBP for cases with large factor sizes. Although

FBP and TRWBP give the same results, the runtime for TRWBP is significantly lower than FBP for many cases.

Figure 11 has the histograms of maximum error in prior marginals obtained with different inference approaches for various benchmarks. Once again, IBIA outperforms other methods with errors less than < 0.1 for BN_UAI and < 0.05 for Grid-BN benchmarks. Max-error with other methods is > 0.5 in quite a few instances in these benchmarks. Although the errors are larger for the relational benchmarks, it still performs better than the other methods. 39% of the instances have maximum errors < 0.05 with IBIA, while the number of such instances is $< 6\%$ for all other methods. Gibbs sampling does not perform well, especially for Grid and Relational benchmarks. For Bnlearn benchmarks, IBIA, WMB and IJGP perform very well due to the larger cluster sizes.

Figure 12 plots the variation of the SumScore obtained using various approximate inference methods as the timeout constraint is varied for different benchmark sets. For the BN_UAI, Grid and Bnlearn, the final score with IBIA, FBP, TRWBP and WMB is similar, indicating that the larger max-errors in the other methods occur only for a small number of states. For these benchmarks, WMB with *ibound* = 10 also achieves a similar score. For Bnlearn, all methods perform well, except for Gibbs sampling which performs very poorly. As discussed earlier, for Bnlearn benchmarks, exact inference is performed with IJGP and WMB because of the *ibound* parameter chosen.

IBIA outperforms other deterministic approximate algorithms by a significant margin in Relational benchmarks. Even though FBP and TRWBP solve more cases than IBIA, the score achieved is small, indicating larger estimation errors. Once again for WMB, the final score is close to the number of cases solved, indicating low average error. WMB with an *ibound* of 10 solves a larger number of cases, but the average error increases as expected. WMB10 has a final score of 226 out of a possible maximum of 242, whereas as WMB with *ibound* of 20 has a score 193 out of a possible maximum of 194. Gibbs sampling performs well in this set of benchmarks, indicating it works better when there is more determinism. For these benchmarks, IJGP does not perform very well both in terms of error and number of cases solved.

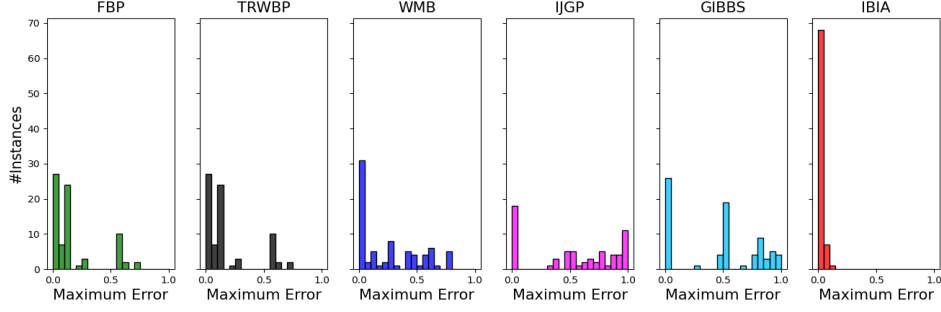
Figure 13 has the distribution of the difference in marginals obtained using FBP, WMB and IJGP and those obtained using IBIA. These are for 29 instances of BN_UAI where ACE does not run but solutions can be obtained using all other methods. We observe that for nearly all variable states, the marginal distribution obtained with IBIA is within ± 0.01 of that obtained with FBP. It is also within ± 0.01 of marginals obtained using WMB and IJGP, in 85% of the cases. The maximum difference in marginals is 0.03 for FBP, 0.2 for WMB and 1.0 for IJGP.

9. Summary, Discussion of results and Conclusions

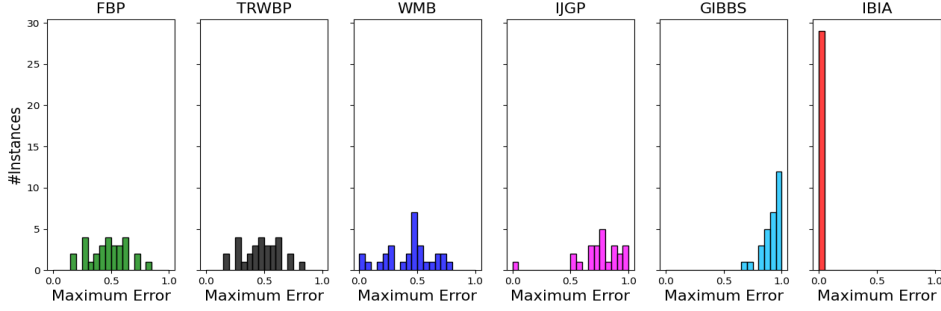
We propose a technique for approximate Bayesian inference that partitions the network based on a user specified parameter mcs_p . For each partition, we incrementally *build* the CT until the clique sizes reach mcs_p , *infer* the clique beliefs using BP, and finally *approximate* the CT to reduce clique sizes to mcs_{im} . The algorithm returns a forest of calibrated CTs corresponding to each partition, as well as the prior beliefs in the absence of evidence and the partition function and a subset of posterior beliefs if evidence is present. A heuris-

Table 10: Comparison of the maximum error, RMSE and the runtime required to obtain prior marginals for BN_UAI. Entries are marked with ‘-’ where inference fails. For consistency in precision across algorithms, the error is reported as zero if accurate to three decimal places.

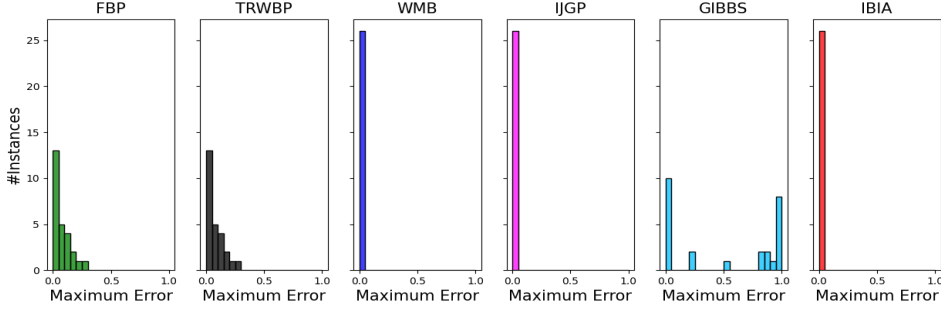
Benchmark	max Error					RMSE					Runtime					
	FBP	TRWBP	WMB	IJGP	IBIA	FBP	TRWBP	WMB	IJGP	IBIA	ACE	FBP	TRWBP	WMB	IJGP	IBIA
BN_105	0.24	0.24	0.197	0.357	0	0.074	0.074	0.057	0.104	0	7	2126	9	344	269	11
BN_107	0.082	0.082	0.209	0.683	0	0.024	0.024	0.084	0.239	0	6	1453	7	294	270	9
BN_109	0.096	0.096	0.122	0.697	0	0.026	0.026	0.028	0.338	0	5	1189	6	328	246	8
BN_111	0.279	0.279	0.284	0.61	0	0.074	0.074	0.085	0.269	0	5	1149	5	307	250	7
BN_113	0.097	0.097	0.095	0.703	0	0.022	0.022	0.027	0.234	0	6	1359	6	294	238	8
BN_115	0.002	0.002	0.038	0.55	0.001	0	0	0.008	0.312	0	429	457	2	370	222	6
BN_117	0.002	0.002	0.052	0.525	0	0	0	0.01	0.327	0	552	920	5	346	234	9
BN_119	0.003	0.003	0.029	0.627	0.001	0.001	0.001	0.005	0.32	0	348	395	2	327	211	5
BN_121	0.001	0.001	0.026	0.501	0.001	0	0	0.005	0.324	0	418	515	3	341	241	6
BN_123	0.001	0.001	0.039	0.655	0.001	0	0	0.007	0.308	0	583	816	4	340	244	7
BN_125	0.001	0.001	0.036	0.534	0.001	0	0	0.009	0.306	0	483	346	2	393	244	5
BN_20	0.15	0.15	0	0	0	0.014	0.014	0	0	0	4515	3	4	166	112	10
BN_21	0.15	0.15	0	0	0.060	0.014	0.014	0	0	0.001	5944	4	4	168	109	11
BN_22	0.271	0.271	0	0	0	0.01	0.01	0	0	0	4	3	3	21	12	5
BN_23	0.271	0.271	0	0	0	0.01	0.01	0	0	0	7	4	3	59	11	5
BN_24	0.702	0.702	0	0	0	0.109	0.109	0	0	0	4	8	9	9	8	4
BN_25	0.702	0.702	0	0	0	0.109	0.109	0	0	0	6	8	10	10	8	3
BN_30	0.606	0.606	0.58	-	0	0.138	0.138	0.156	-	0	93	0.1	0.1	770	-	4
BN_31	0.606	0.606	0.64	0.74	0	0.138	0.138	0.138	0.265	0	65	0.1	0.1	871	552	4
BN_32	0.558	0.558	0.615	-	0	0.152	0.152	0.16	-	0	143	0.1	0.2	940	-	5
BN_33	0.558	0.558	0.657	0.997	0	0.152	0.152	0.156	0.301	0	96	0.1	0.2	992	742	5
BN_34	0.558	0.558	0.556	-	0	0.152	0.152	0.162	-	0	900	0.1	0.2	955	-	5
BN_35	0.558	0.558	0.788	-	0	0.152	0.152	0.168	-	0	276	0.1	0.2	924	-	5
BN_36	0.558	0.558	0.622	-	0	0.152	0.152	0.186	-	0	845	0.1	0.2	1013	-	5
BN_37	0.558	0.558	0.645	-	0.002	0.152	0.152	0.183	-	0	1316	0.1	0.2	1086	-	5
BN_38	0.558	0.558	0.628	-	0	0.152	0.152	0.172	-	0	798	0.1	0.2	964	-	5
BN_39	0.558	0.558	0.648	0.807	0.001	0.152	0.152	0.173	0.262	0	2820	0.1	0.2	1085	740	5
BN_40	0.558	0.558	0.599	-	0.001	0.152	0.152	0.161	-	0	66	0.1	0.2	1113	-	5
BN_41	0.558	0.558	0.599	-	0.001	0.152	0.152	0.173	-	0	202	0.1	0.2	1000	-	5
BN_42	0.072	0.072	0.122	0.75	0.030	0.026	0.026	0.027	0.111	0.001	508	0.01	0.04	91	74	1
BN_43	0.072	0.072	0.113	0.75	0.004	0.026	0.026	0.032	0.115	0	723	0.01	0.04	95	74	2
BN_44	0.072	0.072	0.104	0.316	0.004	0.026	0.026	0.024	0.056	0	677	0.01	0.04	103	69	1
BN_45	0.072	0.072	0.126	0.75	0.004	0.026	0.026	0.039	0.137	0	416	0.01	0.04	81	75	1
BN_46	0.022	0.022	0.239	0.5	0	0.003	0.003	0.036	0.207	0	39	0.01	0.01	109	91	1
BN_47	0.125	0.125	0.271	0.969	0.028	0.017	0.017	0.084	0.353	0.003	1	0.1	0.04	675	557	4
BN_48	0.125	0.125	0.286	0.938	0.030	0.017	0.017	0.088	0.307	0.002	1	0.1	0.05	771	531	3
BN_49	0.125	0.125	0.274	0.969	0.046	0.017	0.017	0.081	0.349	0.003	1	0.1	0.04	650	526	3
BN_50	0.125	0.125	0.298	0.969	0.022	0.017	0.017	0.098	0.337	0.002	1	0.1	0.04	677	553	3
BN_51	0.125	0.125	0.299	0.969	0.034	0.017	0.017	0.096	0.334	0.003	1	0.1	0.04	820	516	3
BN_52	0.125	0.125	0.256	0.953	0.019	0.017	0.017	0.087	0.323	0.002	1	0.1	0.04	738	602	3
BN_53	0.103	0.103	0.452	0.992	0.022	0.018	0.018	0.147	0.299	0.002	1	0.01	0.03	495	413	3
BN_54	0.103	0.103	0.445	0.992	0.044	0.018	0.018	0.135	0.305	0.005	1	0.01	0.03	436	307	3
BN_55	0.103	0.103	0.477	0.992	0.026	0.018	0.018	0.135	0.327	0.002	1	0.02	0.03	439	414	3
BN_56	0.103	0.103	0.453	-	0.044	0.018	0.018	0.13	-	0.005	1	0.03	0.03	572	-	4
BN_57	0.103	0.103	0.42	0.992	0.044	0.018	0.018	0.123	0.302	0.003	1	0.01	0.03	508	395	3
BN_58	0.103	0.103	0.416	0.938	0.044	0.018	0.018	0.128	0.322	0.003	2	0.01	0.02	484	403	3
BN_59	0.125	0.125	0.449	0.938	0.012	0.018	0.018	0.134	0.298	0.001	1	0.02	0.03	568	396	5
BN_60	0.125	0.125	0.457	-	0.070	0.018	0.018	0.143	-	0.006	2	0.02	0.03	550	-	3
BN_61	0.141	0.141	0.337	0.891	0.036	0.017	0.017	0.082	0.324	0.003	0	0.1	0.04	707	558	4
BN_62	0.141	0.141	0.287	0.891	0.056	0.017	0.017	0.085	0.329	0.004	1	0.1	0.05	709	540	3
BN_63	0.125	0.125	0.442	0.938	0.072	0.018	0.018	0.137	0.319	0.003	2	0.02	0.03	486	465	4
BN_64	0.125	0.125	0.504	0.992	0.011	0.018	0.018	0.146	0.337	0.001	2	0.02	0.03	553	404	3
BN_65	0.133	0.133	0.763	0.75	0.070	0.013	0.013	0.248	0.196	0.004	1	0.01	0.01	401	278	4
BN_66	0.133	0.133	0.765	0.875	0.113	0.013	0.013	0.243	0.216	0.007	1	0.01	0.01	385	296	5
BN_67	0.133	0.133	0.771	0.875	0.088	0.013	0.013	0.246	0.208	0.006	1	0.01	0.01	382	336	4
BN_68	0.133	0.133	0.787	0.75	0.096	0.013	0.013	0.256	0.202	0.006	3	0.01	0.01	383	343	4
BN_86	0	0	0	0.487	0	0	0	0	0.03	0	34	77	2	227	133	2
BN_87	0	0	0	0.487	0	0	0	0	0.03	0	51	63	2	229	126	2
BN_88	0	0	0	0.487	0	0	0	0	0.03	0	34	52	2	213	131	2
BN_89	0	0	0	0.487	0	0	0	0	0.03	0	53	114	2	242	114	3
BN_90	0	0	0	0.5	0	0	0	0	0.038	0	36	77	2	214	124	2
BN_91	0	0	0	0.357	0	0	0	0	0.018	0	49	128	2	202	123	2
BN_92	0	0	0.005	0.357	0	0	0	0	0.018	0	34	70	2	186	123	3
BN_93	0	0	0	0.487	0	0	0	0	0.03	0	52	76	2	304	149	3
Mean	0.201	0.201	0.302	0.647	0.018	0.043	0.043	0.086	0.203	0.001						



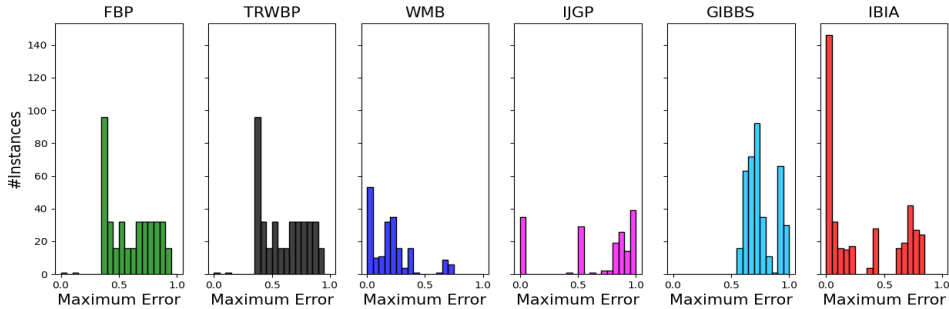
(a) BN_UAI (Instances - #ACE/FBP/TRWBP/GIBBS/WMB/IBIA:76, IJGP:65)



(b) gridBN (Instances - #ACE/FBP/TRWBP/GIBBS/WMB/IBIA:29, IJGP:24)

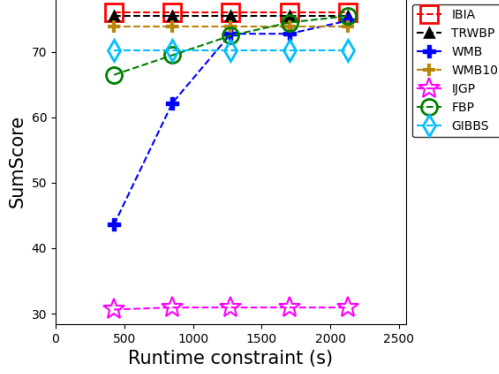


(c) bnlearn (Instances - #ACE/FBP/TRWBP/GIBBS/WMB/IJGP/IBIA:26)



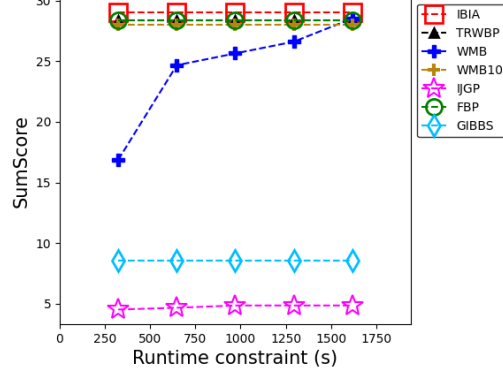
(d) Relational (Instances - #ACE/FBP/TRWBP/GIBBS/IBIA:386, WMB:194, IJGP:168)

Figure 11: Histogram of maximum error in prior node marginals estimated with various approximate inference techniques. The total number of instances that run with ACE and other approximate inference techniques are indicated for each benchmark set. Bin-size=0.05



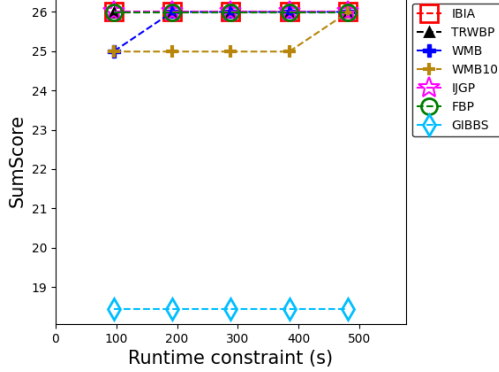
(a) BN_UAI

(Instances - #ACE/FBP/TRWBP/GIBBS/IBIA: 76,
#WMB/WMB10: 76, IJGP: 65)



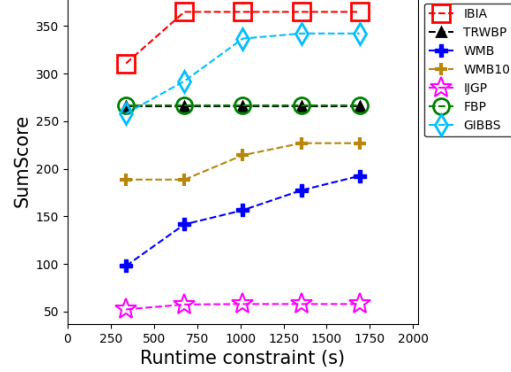
(b) Grid-BN

(Instances - #ACE/FBP/TRWBP/GIBBS/IBIA: 29,
WMB/WMB10: 29, IJGP: 24)



(c) Bnlearn

(Instances - #ACE/FBP/TRWBP/GIBBS/IBIA: 26
#WMB/WMB10/IJGP: 26)



(d) Relational

(Instances - #ACE/FBP/TRWBP/GIBBS/IBIA: 386,
WMB: 194, WMB10: 242, IJGP: 168)

Figure 12: Variation of the *SumScore* for prior marginals obtained using various approximate inference techniques with different timeout constraints. The total number of instances that run with ACE and other approximate inference techniques are indicated for each benchmark set.

tic back propagation algorithm is used to estimate remaining posterior beliefs. We show that our algorithm for incremental construction of CTs always results in a valid CT and our approximation algorithm maintains consistency of within-clique beliefs. The trade-off between runtime and accuracy can be achieved easily in terms of a single user-specified parameter mcs_p . Our method gives significantly smaller errors with competitive runtimes when compared with other approximate methods that have a similar trade-off. Also, unlike other approaches, our method is non-iterative; thus, eliminating the dependence of inference on parameters like the number of iterations, convergence limits, and damping (relaxation) factor.

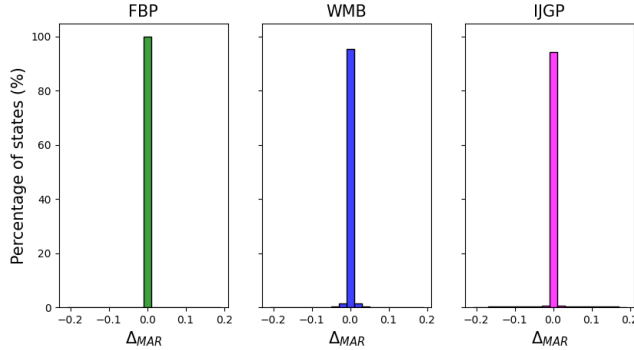


Figure 13: Distribution of difference in prior node marginals ($\Delta_{MAR} = MAR_{IBIA} - MAR_{Alg}$) for BN_UAI testcases (29 instances) where exact marginals cannot be computed using the ACE. Bin-size=0.02

Except for a few cases with strong local structure (like the Grid benchmarks), the maximum clique size obtained using our incremental CT construction algorithm is within ± 2 of what is obtained using complete triangulation of the partition using variable elimination with the min-fill heuristic. This is generally true upto a clique size of 25. As the clique sizes increase beyond this, the differences increase. However, the exponential time and space complexity of inference begins to dominate around these clique sizes, so it is not clear that larger clique sizes are useful. It is also possible to use a combination of incremental and full triangulation if larger clique sizes are desired.

IBIA gives much better estimates of PR than all the other approximate methods. The errors in the estimates are orders of magnitude lower than the other methods. For MAR_e and MAR_p , the max-error and RMSE are significantly lower than all the other approximate methods, even though IJGP and WMB have comparable or better cluster sizes. The *SumScore* is comparable to or better than WMB. This is a reflection of the quality of our approximation algorithm. During “forward propagation” our approximation algorithm maintains within-clique belief consistency, which also gives good estimates of posterior beliefs once all the evidence variables are incorporated. The belief-update via back propagation is heuristic and has some limitations. It is sequential and has to be done link by link for each partition which needs to be updated. Each link update also has a round of message passing. If a belief is erroneously updated from a non-zero value to zero in an intermediate update step, it cannot recover after subsequent updates. This could give rise to errors in the normalization constant if the clique containing that particular belief is updated via a link. This happens occasionally and can be resolved either by not using this link for update or setting it to a small non-zero value. Also as mentioned, after the update is completed, beliefs of variables present in multiple partitions need not be consistent. However, if the belief is obtained from the first partition in which it is added, we get good accuracies. In spite of these limitations, we get significantly better estimates of posteriors than other approximate algorithms used for comparison in this paper (see Table 11 in Appendix, that has results of some more algorithms).

In our method, the trade-off between accuracy and runtime is controlled easily by two user-defined parameters: mcs_p and mcs_{im} . In that respect, it is similar to WMB and IJGP, that has a user defined *ibound* parameter which is similar to mcs_p . This simple control of the trade-off is not possible in most iterative BP algorithms. While it is clear that increasing mcs_p typically improves accuracy at the cost of runtime, the behavior with respect to mcs_{im} is less definitive. Generally, reducing mcs_{im} increases errors due to more aggressive approximations. However, in some cases, the number of partitions reduces, resulting in a slightly lower error. The behaviour of the error with the number of partitions is also network dependent. Even if there are a large number of partitions, the error can be very low or even zero, if the network structure allows a sufficient number of exact marginalizations. For example, the max-error is only 0.049 for the diabetes benchmark with 23 partitions (refer Table 2). Another advantage that IBIA shares with IJGP is that exact inference is automatically performed when the clique sizes are less the specified maximum, which is once again not possible in many region-graph based methods. This property is especially effective when a large number of evidence variables are present.

The run times for various algorithms cannot be compared directly, since they are written in different languages. Moreover, our algorithm is developed in Python and all the other algorithms are compiled programs in Java or C++. In spite of this, the run times for our algorithm are very competitive. We get much better run times than IJGP and WMB, but this is also due to the setting of the *ibound* parameter, which was set as 20 for both these algorithms to allow for a reasonably fair comparison of error. Our algorithm was at a disadvantage in this regard, for networks that have variables that have large domain cardinality or many parents. Interestingly, in these networks (like BN_UAI 105-125), IBIA outperforms FBP in terms of runtime and it's runtime is comparable to that of TRWBP, even though we have clique sizes of 20 and our code is written in Python. In many cases, it is also comparable or better than the run-time of ACE. As seen from Table 11, the other approximate algorithms take longer.

FBP solves the largest number of problems, closely followed by IBIA. However, in all cases, we get better scores and lower errors than FBP. In iterative BP algorithms, there are no convergence guarantees. For IBIA, we can give some guarantees, if mcs_p and mcs_{im} are "CPD-size" aware. When there are no evidence variables, IBIA is guaranteed to give a result under the following conditions:

- mcs_p is large enough to accommodate the variable with the the largest number of states in CPD of a node.
- mcs_{im} is a soft constraint that can be reduced to take into account variables with large number of states.

This is possible, since without evidence, we do not have the constraint that a connected CT should remain connected after the approximation. If we get large cliques containing only interface variables that cannot be approximated using local marginalization, the least correlated interface variables are removed from the clique and added to the CTF as independent nodes. The algorithm is therefore guaranteed to terminate, albeit with a larger error.

In the presence of evidence, no such guarantees can be provided. This is because, in this case, a connected CT should remain connected while forming the partitions. That

said, out of 500+ testcases attempted in this work, we get this error for only five testcases with $mcs_p = 20$ (since it is large enough to accommodate CPDs with large domain sizes). For these cases, we were able to obtain a solution by lowering the mcs_{im} , but this is not guaranteed in general.

IBIA times out while building the CT for partitions in some very large relational BNs (Friends & Smokers). These networks contain numerous evidence states that force equivalence of parent nodes. So far, we have not included such simplifications in our method. However, in large networks without determinism, this could be a constraint. A mix of full and incremental recompilation could possibly work better in these cases.

Finally, our framework can be very useful when portions of the network are changed as well as for BN learning. Since our CT construction method is incremental, portions of the network that have been modified can be deleted and the CT reconstructed without recompiling the entire network. If new evidence variables need to be incorporated, the corresponding partitions can be modified. If a new evidence variable and query are in the same partition, the simplification and inference can be done on that partition alone. In the context of learning, a problem is to learn networks that have a bound on the clique size (Elidan & Gould, 2008; Scanagatta et al., 2018). When the whole network is considered, this places severe restrictions on the number of edges that can be included. Our method can be used to relax some of these constraints and learn partitions of the network.

10. Appendix

Several variants of Belief Propagation and sampling methods have been implemented in the LibDAI library (Mooij, 2010a). We evaluated the performance of the following methods for the BN_UAI benchmark set:

1. Loop Corrected Belief Propagation (LCBP) (Mooij & Kappen, 2007)
2. Conditional Belief Propagation (CBP) (Eaton & Ghahramani, 2009)
3. Tree Expectation Propagation (TREEEP) (Minka & Qi, 2004)
4. Tree Re-weighted Belief Propagation (TRWBP) (Wainwright et al., 2003)
5. Fractional Belief Propagation (FBP) (Wiegerinck & Heskes, 2003)
6. Single-loop Generalized Belief Propagation (GBP) (Yedidia et al., 2005)
with $\text{loopdepth} = 5$
7. Double-loop GBP (HAK) (Heskes, Albers, & Kappen, 2003): with two variants: minimum clusters (HAK_MIN) and $\text{loopdepth} = 3$ (HAK_LOOP3)
8. Gibbs sampling (Gelfand, 2000) with number of vectors = 10^4 , 10^6

Table 11 contains the number of testcases solved within a one-hour runtime limit, max-error, RMSE in MAR_e and error in PR averaged over all benchmarks and the average runtime per benchmark. This experiment was conducted on BN_UAI testcases where the exact probabilities can be computed using ACE. While CBP and LCBP give the least average max-error, they solve only a very few instances (21, 10 out of 90 instances). Similar errors are obtained with different variants of loopy belief propagation like TREEEP, TRWBP and FBP. While single-loop GBP runs successfully for only five testcases, the double-loop variant

HAK runs for a comparable number of testcases and gives similar errors as compared to LBP variants. However, the runtime required is much larger. The Gibbs sampling approach solves most problems with the set time limit. Similar errors were obtained with the number of vectors set to 10^4 and 10^6 .

Based on these results, we chose two variants of LBP namely, TRWBP and FBP for comparison with IBIA.

Table 11: Evaluation of inference algorithms in LibDAI for BN_UAI testcases where exact probabilities can be inferred using ACE. Entries are marked with ‘-’ if the method doesn’t estimate PR .

Total number of instances: 90, $|\Delta_{PR}| = |\log PR_{Alg} - \log PR_{ACE}|$

Algorithm	#Testcases	Avg MaxError	Avg RMSE	Avg $ \Delta_{PR} $	Avg Runtime
LCBP	10	0.039	0.015	-	1350
CBP	21	0.017	0.003	-	67
TREEEP	77	0.194	0.039	0.265	290
TRWBP	87	0.198	0.035	0.237	3
FBP	90	0.207	0.037	0.267	32
GBP_LOOP5	5	0.704	0.242	7.172	315
HAK_MIN	73	0.221	0.038	0.305	477
HAK_LOOP3	63	0.258	0.054	1.717	465
GIBBS - 10^6	88	0.401	0.139	-	554
GIBBS - 10^4	90	0.420	0.140	-	6

References

- Agrawal, D., Pote, Y., & Meel, K. S. (2021). Partition function estimation: A quantitative study. In *Proceedings of the Thirtieth International Joint Conference on Artificial Intelligence, IJCAI-21*, pp. 4276–4285. Survey Track.
- Bathla, S., & Vasudevan, V. (2021). A memory constrained approximate bayesian inference approach using incremental construction of clique trees. TechRxiv. <https://doi.org/10.36227/techrxiv.14938275.v1>.
- Chavira, M., & Darwiche, A. (2005). Compiling bayesian networks with local structure. In *Proceedings of the 19th International Joint Conference on Artificial Intelligence*, Vol. 5, pp. 1306–1312.
- Chavira, M., & Darwiche, A. (2008). On probabilistic inference by weighted model counting. *Artificial Intelligence*, 172(6-7), 772–799.
- Chavira, M., & Darwiche, A. (2015). Ace version 3.0. <http://reasoning.cs.ucla.edu/ace/>. Accessed: 2021-10-15.
- Chavira, M., Darwiche, A., & Jaeger, M. (2006). Compiling relational bayesian networks for exact inference. *International Journal of Approximate Reasoning*, 42(1-2), 4–20.
- Choi, A., Chan, H., & Darwiche, A. (2005). On bayesian network approximation by edge deletion. In *Proceedings of the Twenty-First Conference on Uncertainty in Artificial Intelligence*.

- Choi, A., & Darwiche, A. (2007). Approximating the partition function by deleting and then correcting for model edges. In *Proceedings of the Twenty-Fourth Conference on Uncertainty in Artificial Intelligence*.
- Choi, A., & Darwiche, A. (2008). Many pairs mutual information for adding structure to belief propagation approximations. In *Proceedings of the 23rd National Conference on Artificial Intelligence - Volume 2*.
- Choi, A., & Darwiche, A. (2006). An edge deletion semantics for belief propagation and its practical impact on approximation quality. In *Proceedings, The Twenty-First National Conference on Artificial Intelligence and the Eighteenth Innovative Applications of Artificial Intelligence Conference*, pp. 1107–1114.
- Choi, A., & Darwiche, A. (2010). Relax, compensate and then recover. In *JSAI International Symposium on Artificial Intelligence*, pp. 167–180.
- Darwiche, A. (1998). Dynamic jointrees. In *Proceedings of the Fourteenth Conference on Uncertainty in Artificial Intelligence*, pp. 97–104.
- Darwiche, A. (2001). Recursive conditioning. *Artificial Intelligence*, 126(1-2), 5–41.
- Dechter, R., & Rish, I. (1997). A scheme for approximating probabilistic inference. In *Proceedings of the Thirteenth Conference on Uncertainty in Artificial Intelligence*.
- Dechter, R. (1999). Bucket elimination: A unifying framework for reasoning. *Artificial Intelligence*, 113(1-2), 41–85.
- Dechter, R. (2006). Uai model files and solutions. https://www.ics.uci.edu/~dechter/software/benchmarks/Mpe_Problme_Sets/. Accessed: 2021-10-15.
- Dechter, R., Kask, K., & Mateescu, R. (2002). Iterative join-graph propagation. In *Proceedings of the Eighteenth Conference on Uncertainty in Artificial Intelligence*, pp. 128–136.
- Dechter, R., & Rish, I. (2003). Mini-buckets: A general scheme for bounded inference. *Journal of the ACM*, 50(2), 107–153.
- Dilkas, P., & Belle, V. (2021). Weighted model counting with conditional weights for bayesian networks. In *Proceedings of the Thirty-Seventh Conference on Uncertainty in Artificial Intelligence*, Vol. 161, pp. 386–396.
- Draper, D. L. (1995). Clustering without (Thinking about) Triangulation. In *Proceedings of the Eleventh Conference on Uncertainty in Artificial Intelligence*, pp. 125–133.
- Dudek, J., Phan, V., & Vardi, M. (2020). Addmc: Weighted model counting with algebraic decision diagrams. In *Proceedings of the AAAI Conference on Artificial Intelligence*, pp. 1468–1476.
- Eaton, F., & Ghahramani, Z. (2009). Choosing a variable to clamp. In *Artificial Intelligence and Statistics*, pp. 145–152.
- Elidan, G., & Gould, S. (2008). Learning bounded treewidth bayesian networks.. *Journal of Machine Learning Research*, 9(12).
- Elidan, G., McGraw, I., & Koller, D. (2006). Residual belief propagation: Informed scheduling for asynchronous message passing. In *Proceedings of the Twenty-Second Conference on Uncertainty in Artificial Intelligence*, pp. 165–173.

- Flores, M. J., Gámez, J. A., & Olesen, K. G. (2002). Incremental Compilation of Bayesian Networks. In *Proceedings of the Nineteenth Conference on Uncertainty in Artificial Intelligence*, pp. 233–240.
- Forouzan, S., & Ihler, A. (2015). Incremental region selection for mini-bucket elimination bounds. In *Proceedings of the Thirty-First Conference on Uncertainty in Artificial Intelligence*, pp. 1–10.
- Frey, B. J., & MacKay, D. (1998). A revolution: Belief propagation in graphs with cycles. In *Advances in Neural Information Processing Systems*, Vol. 10.
- Gelfand, A. E. (2000). Gibbs sampling. *Journal of the American statistical Association*, 95(452), 1300–1304.
- Gelfand, A. E., & Welling, M. (2012). Generalized belief propagation on tree robust structured region graphs. In *Proceedings of the Twenty-Eighth Conference on Uncertainty in Artificial Intelligence*, pp. 296–305.
- Gogate, V., & Dechter, R. (2011). Samplesearch: Importance sampling in presence of determinism. *Artificial Intelligence*, 175(2), 694–729.
- Hazan, T., Peng, J., & Shashua, A. (2012). Tightening fractional covering upper bounds on the partition function for high-order region graphs. In *Proceedings of the Twenty-Eighth Conference on Uncertainty in Artificial Intelligence*, pp. 356–366.
- Heskes, T. (2003). Stable fixed points of loopy belief propagation are local minima of the bethe free energy. In *Advances in Neural Information Processing Systems*, Vol. 15.
- Heskes, T. (2006). Convexity arguments for efficient minimization of the bethe and kikuchi free energies. *Journal of Artificial Intelligence Research*, 26, 153–190.
- Heskes, T., Albers, K., & Kappen, B. (2003). Approximate inference and constrained optimization. In *Proceedings of the Nineteenth Conference on Uncertainty in Artificial Intelligence*, pp. 313–320.
- Ihler, A. (2006). Uai model files and solutions. <http://sli.ics.uci.edu/~ihler/uai-data/>. Accessed: 2021-10-15.
- Kask, K., Gelfand, A., Otten, L., & Dechter, R. (2011). Pushing the power of stochastic greedy ordering schemes for inference in graphical models. In *Proceedings of the Twenty-Fifth AAAI Conference on Artificial Intelligence*.
- Kikuchi, R. (1951). A theory of cooperative phenomena. *Physical review*, 81(6), 988.
- Koller, D., & Friedman, N. (2009). *Probabilistic graphical models: principles and techniques*. MIT press.
- Kuck, J., Chakraborty, S., Tang, H., Luo, R., Song, J., Sabharwal, A., & Ermon, S. (2020). Belief propagation neural networks. In *Advances in Neural Information Processing Systems*, Vol. 33, pp. 667–678.
- Lauritzen, S. L., & Spiegelhalter, D. J. (1988). Local computations with probabilities on graphical structures and their application to expert systems. *Journal of the Royal Statistical Society: Series B (Methodological)*, 50(2), 157–194.

- Lee, J., Marinescu, R., Ihler, A., & Dechter, R. (2020). A weighted mini-bucket bound for solving influence diagram. In *Proceedings of The 35th Uncertainty in Artificial Intelligence Conference*, Vol. 115, pp. 1159–1168.
- Lin, P., Neil, M., & Fenton, N. (2020). Improved high dimensional discrete bayesian network inference using triplet region construction. *Journal of Artificial Intelligence Research*, 69, 231–295.
- Liu, Q., & Ihler, A. (2011). Bounding the partition function using holder’s inequality. In *Proceedings of the 28th International Conference on Machine Learning*, pp. 849–856.
- Marinescu, R. (2016). Merlin. <https://github.com/radum2275/merlin/>. Accessed: 2021-10-15.
- Mateescu, R., Kask, K., Gogate, V., & Dechter, R. (2010). Join-graph propagation algorithms. *Journal of Artificial Intelligence Research*, 37, 279–328.
- Minka, T., & Qi, Y. (2004). Tree-structured approximations by expectation propagation. *Advances in Neural Information Processing Systems*, 16, 193–200.
- Minka, T. P. (2001). Expectation propagation for approximate bayesian inference. In *Proceedings of the Seventeenth Conference on Uncertainty in Artificial Intelligence*, pp. 362–369.
- Minka, T. (2004). Power ep. Tech. rep. MSR-TR-2004-149, Microsoft Research Ltd.
- Minka, T. (2005). Divergence measures and message passing. Tech. rep. MSR-TR-2005-173, Microsoft Research Ltd.
- Mooij, J. M. (2010a). libDAI: A free and open source C++ library for discrete approximate inference in graphical models. *Journal of Machine Learning Research*, 11, 2169–2173.
- Mooij, J. M. (2010b). Reference manual for libDAI: A free and open source C++ library for discrete approximate inference in graphical models. <https://staff.fnwi.uva.nl/j.m.mooij/libDAI/doc/>. Accessed: 2021-10-15.
- Mooij, J. M., & Kappen, H. J. (2007). Loop corrections for approximate inference on factor graphs. *Journal of Machine Learning Research*, 8(40), 1113–1143.
- Murphy, K. P., Weiss, Y., & Jordan, M. I. (1999). Loopy belief propagation for approximate inference: An empirical study. In *Proceedings of the Fifteenth Conference on Uncertainty in Artificial Intelligence*, pp. 467–475.
- Olesen, K. G., & Madsen, A. L. (2002). Maximal prime subgraph decomposition of bayesian networks. *IEEE Transactions on Systems, Man, and Cybernetics, Part B: Cybernetics*, 32(1), 21–31.
- Rollon, E., & Dechter, R. (2010). New mini-bucket partitioning heuristics for bounding the probability of evidence. In *Proceedings of the AAAI Conference on Artificial Intelligence*, pp. 1199–1204.
- Roth, D. (1996). On the hardness of approximate reasoning. *Artificial Intelligence*, 82(1-2), 273–302.
- Sang, T., Beame, P., & Kautz, H. A. (2005). Performing bayesian inference by weighted model counting. In *Proceedings of the 20th National Conference on Artificial Intelligence - Volume 1*, Vol. 5, pp. 475–481.

- Scanagatta, M., Corani, G., De Campos, C. P., & Zaffalon, M. (2018). Approximate structure learning for large bayesian networks. *Machine Learning*, 107(8), 1209–1227.
- Schult, D. A., & Swart, P. (2008). Exploring network structure, dynamics, and function using networkx. In *Proceedings of the 7th Python in science conferences (SciPy 2008)*, Vol. 2008, pp. 11–16.
- Scutari, M. (2007). Bayesian network repository. <https://www.bnlearn.com/bnrepository/>. Accessed: 2021-10-15.
- Shenoy, P. P., & Shafer, G. (1986). Propagating belief functions with local computations.. *IEEE Expert*, 1(3), 43–52.
- Sontag, D., Meltzer, T., Globerson, A., Jaakkola, T., & Weiss, Y. (2008). Tightening lp relaxations for map using message passing. In *Proceedings of the Twenty-Fourth Conference on Uncertainty in Artificial Intelligence*, pp. 503–510.
- Wainwright, M. J., Jaakkola, T. S., & Willsky, A. S. (2003). Tree-reweighted belief propagation algorithms and approximate ml estimation by pseudo-moment matching. In *International Workshop on Artificial Intelligence and Statistics*, pp. 308–315.
- Welling, M. (2004). On the choice of regions for generalized belief propagation. In *Proceedings of the 20th Conference on Uncertainty in Artificial Intelligence*, pp. 585–592.
- Welling, M., Minka, T., & Teh, Y. W. (2005). Structured region graphs: Morphing ep into gbp. In *Proceedings of the Twenty-First Conference on Uncertainty in Artificial Intelligence*.
- Wiegerinck, W., & Heskes, T. (2003). Fractional belief propagation. In *Advances in Neural Information Processing Systems*, Vol. 15.
- Winn, J., Bishop, C. M., & Jaakkola, T. (2005). Variational message passing.. *Journal of Machine Learning Research*, 6(4).
- Xiang, Y., & Lesser, V. (2003). On the role of multiply sectioned bayesian networks to co-operative multiagent systems. *IEEE Transactions on Systems, Man, and Cybernetics-Part A: Systems and Humans*, 33(4), 489–501.
- Xiang, Y., Poole, D., & Beddoes, M. P. (1993). Multiply sectioned bayesian networks and junction forests for large knowledge-based systems. *Computational Intelligence*, 9(2), 171–220.
- Yedidia, J. S., Freeman, W. T., & Weiss, Y. (2005). Constructing free-energy approximations and generalized belief propagation algorithms. *IEEE Transactions on information theory*, 51(7), 2282–2312.
- Yedidia, J. S., Freeman, W. T., Weiss, Y., et al. (2000). Generalized belief propagation. In *Advances in Neural Information Processing Systems*, Vol. 13, pp. 689–695.
- Yuille, A. L., & Rangarajan, A. (2002). The concave-convex procedure (cccp). In *Advances in Neural Information Processing Systems*, Vol. 14.